OFFICE OF CIVILIAN RADIOACTIVE WASTE MANAGEMENT

QA: QA

ERRATA

1. TER No. TER-03-0023

DC Tracking No. 36176

2. Product DI:	Title:	Revision:
MDL-NBS-HS-000003 (U0035)	Calibrated Properties Model	Rev 01

3. Location	4. Clarification/Restriction
Section 6, Table 5:	The Scientific Notebook ID number is listed as SN-LBNL-SCI-299-V1 instead of the correct one SN-LBNL-SCI-229-V1.
Correct the RPC submittal for the records package for Wang 2002[160401]:	The records package for Wang 2002[160401] has been corrected to indicate the corrected Scientific Notebook ID number SN-LBNL-SCI-229-V1.
Section 4.1.2.1, p. 20, Table 4, second row from bottom:	"tcwf" to be corrected to "tswf"; and the alpha value of "3.2E-4" to be corrected to "3.2E-3". see output DTN LB0207RevUZ FRP.001 SRH 6/24/03
Section 6.3.3, p. 53, Table 15.	The basecase value for the model layer ptn21 is incorrectly listed as "2.11E-11" instead of "2.11E-12". see output DTN LB02091DSSCP3I. 002 SRH 6/24/03 No IRANs have been initiated. These typographycal errors do not affect the product output data submitted to the TDMS; these submittals do not contain the errors.

5. QER Review: (Print Name) Stephen Harris	Initials: SRH	Date: 6/24/03
6. Responsible Manager: (Print Name) Joseph J. WANG	Initials: JW	Date: 6/24/03

OFFICE OF CIVILIAN RADIOACTIVE WASTE MANAGEMENT
MODEL COVER SHEET

1. QA: QA

Page: 1 of: 82

Complete Only Applicable Items

2. Type of Mathematical Model

[x] Process Model [ ] Abstraction Model [ ] System Model

Describe Intended Use of Model:
The developed calibrated properties are used in process models to simulate flow and transport in the UZ for performance assessment.

Technical Contact/Department:
J. Houseworth/Unsaturated Zone Flow, Transport, and Coupled Processes

3. Title:
Calibrated Properties Model

4. DI (Including Rev. No. and Change No., if applicable):
MDL-NBS-HS-000003 REV01

5. Total Attachments:	6. Attachment Numbers - No. of Pages in Each:
1	I-5

	Printed Name	Signature	Date
7. Originator	H.H. Liu	SIGNATURE ON FILE	2-14-03
8. CSO	M. Zhu	SIGNATURE ON FILE	02/14/03
9. Checker	P. Persoff	SIGNATURE ON FILE	02/14/03
10. QER	S. Harris	SIGNATURE ON FILE	02/14/03
11. Responsible Manager/ Lead	Y-S. Wu	SIGNATURE ON FILE	02/14/03
12. Responsible Manager	J.S.Y. Wang	SIGNATURE ON FILE	02/14/03

13. Remarks:

Block 7. Prepared by H.H. Liu with C.F. Ahlers contributing to Section 6 and L. Pan contributing to Section 7. Y-S. Wu also contributed to Section 6.3.4.

2. Model Title:
Calibrated Properties Model

3. DI (including Rev. No. and Change No., if applicable):
MDL-NBS-HS-000003 REV01

4. Revision/Change No.	5. Description of Revision/Change
00	Initial Issue
00 01	This ICN resolves TBV numbers 0536 and 4755 by replacing citations of TBV Data Tracking Numbers (DTNs) with qualified and verified DTNs having the same parameter values. This action does not affect or alter input or output values and conclusions in the anlysis. The following DTNs were affected: DTN: GS000399991221.004 is replaced with DTN: MO0109HYMXPROP.001 DTN: GS960208312261.001 is replaced with DTN: GS000608312261.001 The Reference Section and DIRS have been updated to accomodate the above changes, to resolve URN numbers, and to update document tracking numbers. Changes in ICN 01 of this AMR are marked with change bars in the document margins. Attachment IV of this technical product contains documentation of single use software routines or macros that were qualified under procedure AP-SI.1Q, Software Management, prior to the release of Rev. 03 of said procedure. As the scope of this ICN did not involve a change to the routine codes, and they have not been used to develop additional quality affecting information in this technical product, these single use software routines or macros will remain documented herein, in accordance with AP-SI.1Q prior to the release of Rev. 03. The following Sections (pages) are affected by this ICN: Section 1 (p. 11), 2 (p. 13), 3 (p. 15), 4 (p.19), 6 (p. 39), 7 (pp. 27, 29-30, 33, 35, 67, 69-70), 8 (pp. 71-75), and Attachment I. Document Input Reference Sheet has been removed from Attachment I.
REV01	Entire model documentation was revised to update the model and calibrated property sets that are compatible with the revised grid and hydrologic property data. Side bars are not used because the changes were too extensive to use Step 5.9d)1) per AP-SIII.10Q/Rev.0/ICN 2.

CONTENTS

CONTENTS (Continued)

LIST OF FIGURES

INTENTIONALLY LEFT BLANK

LIST OF TABLES

INTENTIONALLY LEFT BLANK

ACRONYMS

1-D	one-dimensional
2-D	two-dimensional
3-D	three-dimensional
AC	Acceptance Criterion
ACC	Accession Number
AMR	Analysis / Model Report
AP	Administrative Procedure (DOE)
BSC	Bechtel SAIC Company, LLC
CFu	Crater Flat undifferentiated hydrogeologic unit
CHn	Calico Hills nonwelded hydrogeologic unit
CRWMS	Civilian Radioactive Waste Management System
DOE	U.S. Department of Energy
DST	Drift-Scale Test
DTN	Data Tracking Number
DIRS	Document Input Reference System
ECRB	Enhanced Characterization of Repository Block
ESF	Exploratory Studies Facility
FY	Fiscal Year
GFM	Geologic Framework Model
HGU	Hydrogeologic Unit
LBNL	Lawrence Berkeley National Laboratory
M&O	Management and Operating Contractor
NSP	Nevada State Plane
OCRWM	Office of Civilian Radioactive Waste Management
ORD	Office of Repository Development
PA	Performance Assessment
PTn	Paintbrush nonwelded hydrogeologic unit

ACRONYMS (Continued)

Q	Qualified
QARD	Quality Assurance Requirements and Description
QIP	Quality Implementing Procedure
RMSE	Root-mean-square error
SCM	Software Configuration Management
STN	Software Tracking Number
TCw	Tiva Canyon welded hydrogeologic unit
TDMS	Technical Data Management System
TSPA	Total System Performance Assessment
THC	Thermal-Hydrological-Chemical
TH	Thermal-Hydrological
TPO	Technical Product Output
TWP	Technical Work Plan
TSw	Topopah Spring welded hydrogeologic unit
USGS	United States Geological Survey
UZ	Unsaturated Zone
UZ Model	Unsaturated Zone Flow and Transport Model
WP	Work Package
YMP	Yucca Mountain Site Characterization Project

1. PURPOSE

The purpose of this Model Report is to document the Calibrated Properties Model that provides calibrated parameter sets for unsaturated zone (UZ) flow and transport process models for the Office of Repository Development (ORD). The UZ contains the unsaturated rock layers overlying the repository and host unit, which constitute a natural barrier to flow, and the unsaturated rock layers below the repository which constitute a natural barrier to flow and transport. This work followed, and was planned in, *Technical Work Plan (TWP) for: Performance Assessment Unsaturated Zone* (BSC 2002 [160819], Section 1.10.8 [under Work Package (WP) AUZM06, Climate Infiltration and Flow], and Section I-1-1 [in Attachment I, Model Validation Plans]). In Section 4.2, four acceptance criteria (ACs) are identified for acceptance of this Model Report; only one of these (Section 4.2.1.3.6.3, AC 3) was identified in the TWP (BSC 2002 [160819], Table 3-1). These calibrated property sets include matrix and fracture parameters for the UZ Flow and Transport Model (UZ Model), drift seepage models, and drift-scale and mountain-scale coupled-process models from the UZ Flow, Transport and Coupled Processes Department in the Natural Systems Subproject of the Performance Assessment (PA) Project. The Calibrated Properties Model output will also be used by the Engineered Barrier System Department in the Engineering Systems Subproject. The Calibrated Properties Model provides input through the UZ Model and other process models of natural and engineered systems to the Total System Performance Assessment (TSPA) models, in accord with the PA Strategy and Scope in the PA Project of the Bechtel SAIC Company, LLC (BSC). The UZ process models provide the necessary framework to test conceptual hypotheses of flow and transport at different scales and predict flow and transport behavior under a variety of climatic and thermal-loading conditions. UZ flow is a TSPA model component.

This Model Report documents the development of the following calibrated property sets, which have been submitted to the Technical Data Management System (TDMS):

- Drift-scale calibrated parameter sets based on one-dimensional inversions (Output-DTN: LB0208UZDSCPMI.002 for base-case infiltration, LB0208UZDSCPUI.002 for upper-bound infiltration, and LB0208UZDSCPLI.002 for lower-bound infiltration)

- Mountain-scale calibrated parameter sets based on one-dimensional inversions (Output-DTN: LB02091DSSCP3I.002)

- Calibrated fault parameters (one set for all three infiltration scenarios) based on two-dimensional inversions (Output-DTN: LB02092DSSCFPR.002)

The objective of the calibration process is to provide calibrated parameter sets for use in process models to simulate flow and transport in the Yucca Mountain UZ for PA. The calibration process includes inversions utilizing the code iTOUGH2 V5.0 (LBNL 2002 [160106]). Note that software routine infil2grid V1.7 (LBNL 2002 [154793]) was not planned in the TWP (BSC 2002 [160819], Table II.2), but used in this report. This is because infil2grid V1.7 (LBNL 2002 [154793]) can handle eight-character grid-element names, while infil2grid V1.6 (LBNL 1999 [134754]) cannot. This and the AC mentioned above are the only deviations from the TWP.

Property sets are generated corresponding to maps of the best estimate of present-day net infiltration, as well as maps representing the expected upper and lower bounds of net infiltration. The caveats and limitations for use of each of these property sets are documented in Section 6.0. The limitations of the Calibrated Properties Model are also discussed in Section 6.0.

This report also addresses the following issues: providing an updated Calibrated Properties Model that incorporates uncertainties from significant sources (Sections 6.2 and 6.4), calibration of the UZ flow model using the most recent data (Sections 6.2 and 6.3.4), providing the basis for the proportion of fracture flow through the Calico Hills nonwelded vitric (Section 6.1), and providing an analysis of available hydrological data used for support of the flow field below the repository (Section 6.3).

This Model Report is the basis for documents that detail UZ Flow Models and Submodels, the Mountain-Scale Coupled Thermal-Hydrological (TH) Process Models, the Mountain-Scale Radionuclide Transport Model, the Drift-Scale Test (DST) Thermal-Hydrological-Chemical (THC) Model, the THC Seepage Model, and the Seepage Model for PA. The UZ Flow Models and Submodels directly support the Features, Events, and Processes screening decisions (BSC 2002 [160819], Table 2–6).

2. QUALITY ASSURANCE

The activities documented in this Model Report were evaluated under Administrative Procedure (AP) AP-2.27Q*, Planning for Science Activities*, and were determined to be subject to the requirements of the U.S. Department of Energy (DOE) Office of Civilian Radioactive Waste Management (OCRWM) *Quality Assurance Requirements and Description* (QARD) (DOE 2002 [159475]). This evaluation is documented in *Technical Work Plan (TWP) for: Performance Assessment Unsaturated Zone* (BSC 2002 [160819], Section 8.2, under Work Package (WP) AUZM06). Electronic management of information was evaluated in accordance with AP-SV.1Q, *Control of the Electronic Management of Information*, and followed and controlled under YMP-LBNL-QIP-SV.0, *Management of YMP-LBNL Electronic Data*.

This Model Report provides calibrated values for hydrologic properties of natural barriers (hydrogeologic units of the UZ) identified in the *Q-List* (YMP 2001 [154817], Section 5). The report contributes to the analyses and modeling data used to support performace assessment. The conclusions of this Model Report do not affect the proposed repository design or permanent items as discussed in AP-2.22Q*, Classification Criteria and Maintenance of the Monitored Geologic Repository Q-List*. Activities documented in this report were conducted in accordance with the quality assurance program using OCRWM APs and YMP-LBNL-QIPs as identified in the TWP (BSC 2002 [160819], Attachment II). This Model Report has been evaluated for accuracy, precision, and representativeness in accordance with AP-SIII.10Q, *Models.*

The document identifier was obtained as per AP-6.1Q, *Document Control*. Input-DTNs were documented in accordance with AP-3.15Q, *Managing Technical Product Inputs.* Data not already in the Technical Data Management System (TDMS) were submitted to the TDMS in accordance with AP-SIII.3Q, *Submittal and Incorporation of Data to the Technical Data Management System.* Software, as applicable, was obtained, controlled, and documented as per AP-SI.1Q, *Software Management.*

Reviews by a Checker and Bechtel SAIC Company, LLC (BSC) Quality Engineering Representative (QER) were conducted per AP-SIII.10Q; Independent Technical and Engineering Assurance reviews were performed per YMP-LBNL-QIP-6.1, *Document Review*; and interdisciplinary reviews were conducted in accordance with AP-2.14Q, *Review of Technical Products and Data*. Upon completion of the checking and review process, this Model Report was approved per AP-SIII.10Q and processed in accordance with AP-6.1Q. The records required by Sections 6.1 and 6.2 of AP-SIII.10Q were collected and submitted to the Records Processing Center in accordance with AP-17.1Q, *Record Source Responsibilities for Inclusionary Records*. The records listed in Section 6.3 of AP-SIII.10Q were dispositioned by the Record Source per requirements in AP-32.4, *Records Retention and Disposition*.

INTENTIONALLY LEFT BLANK

3. USE OF SOFTWARE

The software programs used in this study are listed in Table 1. These are appropriate for the intended application and were used only within the range of validation. They were obtained from Software Configuration Management (SCM), and qualified under AP-SI.1Q, *Software Management.*

Table 1. Qualified Software Used in This Report

Software Name	Version	Software Tracking Number (STN)	Document Input Reference System (DIRS) ID
iTOUGH2	5.0	10003-5.0-00	160106
infil2grid	1.6	10077-1.6-00	134754
infil2grid	1.7	10077-1.7-00	154793
aversp_1	1.0	10878-1.0-00	146533
TBgas3D	2.0	10882-2.0-00	160107
e9-3in	1.0	10126-1.0-00	146536

Standard Excel spreadsheets and visual display graphics programs (Excel 97 SR-1 and Tecplot V7.0) were also used but are not subject to software quality assurance requirements. All information needed to reproduce the work using these standard software programs, including the input, computation, and output, is included in this report (Attachment I). All computations are described by title in Sections 6 and 7 with reference to Attachment I.

INTENTIONALLY LEFT BLANK

4. INPUTS

4.1 DATA AND PARAMETERS

Source information on the data and parameter inputs is summarized in Table 2 and is further documented below. The appropriateness of the input data and parameters is also described.

4.1.1 Output from Other Models and Analyses

Developed data include the spatially varying infiltration maps from the Infiltration Model and several numerical grids, which are documented in separate reports (USGS 2001 [160355]; BSC 2003 [160109]). These data sets are too large to reproduce here, but are listed by DTN in Table 2. Uncalibrated matrix and fracture properties and property-estimate uncertainty data (e.g., standard deviation and number of samples) that are used as input to the calibration are listed in Tables 3 and 4. Porosity, residual saturation, satiated saturation, and van Genuchten parameter *m* are not calibrated. All other properties and uncertainty data are used to constrain the calibration. The infiltration maps are the currently available best estimates of infiltration rate distributions for UZ. The appropriateness of the numerical grids for modeling flow and transport in UZ is presented in a scientific analysis report (BSC 2003 [160109]).

4.1.2 Acquired Data

Acquired data include saturation, water potential, and pneumatic pressure. In all cases, the data sets are too large to reproduce here, but are listed by DTN in Table 2. These data are developed prior to use in the inversions as documented in Sections 6.2 and 6.3.4. Data that are not used are also discussed.

4.1.2.1 Saturation Data

Saturation data measured on core from boreholes USW SD-6, USW SD-7, USW SD-9, USW SD-12, USW UZ-14, UE-25 UZ#16, USW WT-24, USW UZ-N11, USW UZ-N31, USW UZ-N 32, USW UZ-N33, USW UZ-N37, USW UZ-N38, USW UZ-N53, USW UZ-N54, USW UZ-N55, USW UZ-N57, USW UZ-N58, USW UZ-N59, and USW UZ-N61 are used for the one-dimensional (1-D) inversions or model validation. The locations of these boreholes are shown in Figure 1. These boreholes do not intersect mapped faults, and thus the saturation data from these boreholes are representative of the rock mass of Yucca Mountain. Saturation data measured on core from borehole USW UZ-7a (location shown in Figure 1) are used for the two-dimensional (2-D) inversions. This borehole intersects the Ghost Dance fault, and saturation data from this borehole are judged to be representative of the faulted rock at Yucca Mountain.

Saturation data measured on core from several boreholes and tunnels at Yucca Mountain are not included in any of the inversions. Saturation data measured on core from boreholes USW NRG-6 and USW NRG-7a are not used because handling of the core caused excessive drying (Rousseau et al. 1999 [102097], p. 125). Saturation data measured on core from the Exploratory Studies Facility (ESF), Enhanced Characterization of Repository Block (ECRB) Cross Drift, alcoves, and niches are not used, because they represent only a single layer in the stratigraphic column. Geophysical measurements of saturation are not used because of larger uncertainties associated

with these data, compared with direct measurements of saturation by oven drying. A detailed discussion of the relevant geophysical measurements was presented in BSC (2002 [160319], Attachment II) as compared with the corresponding core-measurements. The geophysical data may be useful for future model calibration activities as corroborative data.

Table 2. Input Data Sources and Data Tracking Numbers

DTN	Data Description	Data Use*
MO0109HYMXPROP.001 [155989]	Saturation data from cores for boreholes USW SD-7, USW SD-9, USW SD-12, USW UZ-14, UE-25 UZ#16, USW UZ-7a, USW WT-24, USW UZ-N11, USW UZ-N31, USW UZ-N32, USW UZ-N33, USW UZ-N37, USW UZ-N38, USW UZ-N53, USW UZ-N54, USW UZ-N55, USW UZ-N57, USW UZ-N58, USW UZ-N59, and USW UZ-N61.	6.2.2 6.3.2
GS980808312242.014 [106748]	Saturation Data from Cores for Borehole USW SD-6	6.2.2 6.3.2
GS980708312242.010 [106752]	Saturation Data from Cores for Borehole USW WT-24	6.2.2 6.3.2
GS950208312232.003 [105572] GS951108312232.008 [106756] GS960308312232.001 [105573] GS960808312232.004 [105974] GS970108312232.002 [105975] GS970808312232.005 [105978] GS971108312232.007 [105980] GS980408312232.001 [105982]	*In situ* Water-Potential Data for Boreholes USW NRG-6, USW NRG-7a, USW SD-12, UE-25 UZ#4, & USW UZ-7a	6.2.2
GS000608312261.001 [155891]	*In situ* Pneumatic Pressure Data for Borehole UE-25 NRG#5	6.2.3
GS950208312232.003 [105572] GS951108312232.008 [106756] GS960308312232.001 [105573] GS960808312232.004 [105974]	*In situ* Pneumatic Pressure Data for Borehole USW NRG-6 & USW NRG-7a	6.2.3
GS960908312261.004 [106784]	*In situ* Pneumatic Pressure Data for Borehole USW SD-7	6.2.3
GS960308312232.001 [105573]	*In situ* Pneumatic Pressure Data for Borehole USW SD-12 & USW UZ-7a	6.2.3 6.3.4
GS000308311221.005 [147613] **	Infiltration Map (modern climate—mean, lower and upper) (USGS 2001 [160355])	6.2.5
LB02081DKMGRID.001 [160108] **	1-D and 2-D Grids (BSC 2003 [160109])	6.2.1
LB0205REVUZPRP.001 [159525]	Uncalibrated Fracture Property Data	6.2.4
LB0207REVUZPRP.002 [159672]	Uncalibrated Matrix Property Data	6.2.4 6.4.1
LB0207REVUZPRP.001 [159526]	Uncalibrated Fault Property Data	6.2.4
LB997141233129.001 [104055] ** LB997141233129.002 [119933] ** LB997141233129.003 [119940] **	Calibrated Basecase Infiltration 1-D Parameter Set for the UZ Flow and Transport Model, FY99, (BSC 2001 [161316]).	6.3.3
LB991091233129.001 [125868] **	One-Dimensional, Mountain-Scale Calibration for Calibrated Properties Model, FY99 (BSC 2001 [161316]).	6.2.2 6.2.5 6.3.2
LB991091233129.003 [119902] **	Two-Dimensional, Fault Calibration for Calibrated Properties Model, FY99 (BSC 2001 [161316])	6.3.4
MO0012MWDGFM02.002 [153777] **	Geologic Framework Model (GFM2000) (BSC 2002 [159124]).	6.2.2 6.2.3
LB02103DPNEUSM.001 [160250] **	3-D Pneumatic Simulations (BSC 2001 [158726]).	7.5
GS940208314211.008 [145581]	Table of Contacts in boreholes USW UZ-N57, N59 and N61.	6.2.2

NOTE: * Sections where the data used is described in detail.
**Technical Product Output (TPO)

Table 3. Uncalibrated Matrix Properties and Uncertainty Data (The relation between hydrogeologic units (HGU) and UZ model layers is given in Table 6.)

HGU	ϕ	k [m^2]	log(k) [log(m^2)]	$\sigma_{log(k)}$	N	N non-detect	$SE_{log(k)}$	$1/\alpha$ [Pa]	log($1/\alpha$) [log(Pa)]	$SE_{log(1/\alpha)}$	m	SE_m	S_r
CCR & CUC	0.241	4.7E-15	-14.33	0.47	3	0	0.27	8.27E+04	4.918	0.279	0.388	0.085	0.02
CUL & CW	0.088	6.4E-20	-19.20	2.74	15	25	0.43	5.46E+05	5.737	0.178	0.280	0.045	0.20
CMW	0.200	1.8E-16	-15.74	2.38	5	1	0.97	2.50E+05	5.398	0.188	0.259	0.042	0.31
CNW	0.387	4.0E-14	-13.40	2.05	10	0	0.65	2.03E+04	4.308	0.199	0.245	0.032	0.24
BT4	0.428	4.1E-13	-12.39	1.41	11	0	0.43	4.55E+03	3.658	0.174	0.219	0.019	0.13
TPY	0.233	1.3E-15	-14.90	0.64	2	0	0.46	7.63E+04	4.883	0.379	0.247	0.064	0.07
BT3	0.413	1.3E-13	-12.87	1.09	11	1	0.31	8.90E+03	3.950	0.088	0.182	0.008	0.14
TPP	0.498	1.1E-13	-12.96	0.39	11	0	0.12	2.12E+04	4.325	0.104	0.300	0.023	0.06
BT2	0.490	6.7E-13	-12.17	1.12	21	0	0.24	1.74E+04	4.239	0.170	0.126	0.013	0.05
TC	0.054	4.4E-17	-16.36	3.02	6	5	0.91	2.71E+05	5.432	0.310	0.218	0.054	0.21
TR	0.157	3.2E-16	-15.50	0.94	46	1	0.14	9.43E+04	4.974	0.116	0.290	0.025	0.07
TUL	0.155	2.8E-17	-16.56	1.61	37	12	0.23	1.75E+05	5.244	0.111	0.283	0.024	0.12
TMN	0.111	4.5E-19	-18.34	0.97	74	35	0.09	1.40E+06	6.147	0.108	0.317	0.042	0.19
TLL	0.131	3.7E-17	-16.44	1.65	51	24	0.19	6.01E+04	4.779	0.521	0.216	0.061	0.12
TM2 & TM1	0.103	2.3E-20	-19.63	3.67	21	42	0.46	3.40E+06	6.532	0.097	0.442	0.073	0.20
PV3	0.043	2.9E-18	-17.54	1.57	16	2	0.37	1.00E+06	6.000	0.278	0.286	0.065	0.42
PV2a	0.275	a	a	a	a	a	a	2.17E+05	5.336	0.156	0.059	0.007	0.36
PV2v	0.229	4.3E-13	-12.37	1.38	16	0	0.34	1.94E+04	4.287	0.042	0.293	0.011	0.13
BT1a	0.285	3.5E-17	-16.45	2.74	9	1	0.87	4.72E+06	6.674	0.183	0.349	0.073	0.38
BT1v	0.331	2.1E-13	-12.67	1.11	35	0	0.19	1.35E+04	4.131	0.049	0.240	0.008	0.06
CHV	0.346	1.6E-12	-11.81	1.62	46	0	0.24	3.39E+03	3.530	0.094	0.158	0.008	0.06
CHZ	0.322	5.2E-18	-17.28	0.91	99	17	0.08	4.45E+05	5.649	0.094	0.257	0.022	0.26
BTa	0.271	8.2E-19	-18.08	2.05	9	8	0.50	6.42E+06	6.808	0.043	0.499	0.036	0.36
BTv	b	b	b	b	b	b	b	5.04E+04	4.703	0.207	0.147	0.020	b
PP4	0.321	1.5E-16	-15.81	2.74	6	2	0.97	5.00E+05	5.699	0.401	0.474	0.224	0.29
PP3	0.318	6.4E-15	-14.20	0.75	51	0	0.11	1.32E+05	5.120	0.084	0.407	0.031	0.08
PP2	0.221	5.4E-17	-16.27	1.18	34	3	0.19	6.22E+05	5.794	0.147	0.309	0.041	0.10
PP1	0.297	8.1E-17	-16.09	1.52	27	1	0.29	1.13E+05	5.052	0.234	0.272	0.036	0.30
BF3/TR3	0.175	1.1E-15	-14.95	1.64	7	1	0.58	8.94E+04	4.951	0.931	0.193	0.117	0.11
BF2	0.234	c	c	c	c	c	c	8.46E+06	6.927	0.032	0.617	0.070	0.21

DTN: LB0207REVUZPRP.002 [159672]

NOTE: (a) BT1a was used as an analog for permeability because only one permeability data point is available for PV2a.
(b) BT1v was used as an analog for porosity, residual saturation, and permeability because only one sample is available for BTv.
(c) PP1 was used as an analog for permeability because only one measurable permeability data point is available for BF2.
k is permeability.
σ is standard deviation.
N is number of samples.
ϕ is porosity.
α and m are fitting parameters for the van Genuchten water potential relationship.
SE is standard error.
S_r is residual liquid saturation.
Non-detect means permeability too low to measure.
BTa and BTv correspond to zeolitic and vitric BT, respectively, in Table 6.

Table 4. Uncalibrated Fracture Property Data

UZ Model Layer	permeability (m^2)				frequency (m^{-1})			van Genuchten			porosity (-)	Std (-)
	k_G	log(k_G)	$\sigma_{log(kG)}$	N	f	σ_f	N	α (Pa^{-1})	log(α)	m (-)		
tcw11	3.0E-11	-10.52	-	2	0.92	0.94	76	5.0E-3	-2.30	0.633	2.4E-2	-
tcw12	5.3E-12	-11.28	0.78	80	1.91	2.09	1241	2.2E-3	-2.66	0.633	1.7E-2	-
tcw13	4.5E-12	-11.35	1.15	3	2.79	1.43	60	1.9E-3	-2.73	0.633	1.3E-2	-
ptn21	3.2E-12	-11.49	0.88	12	0.67	0.92	76	2.7E-3	-2.57	0.633	9.2E-3	-
ptn22	3.0E-13	-12.52	0.20	4	0.46	-	-	1.4E-3	-2.86	0.633	1.0E-2	-
ptn23	3.0E-13	-12.52	0.20	4	0.57	-	63	1.2E-3	-2.91	0.633	2.1E-3	-
ptn24	3.0E-12	-11.52	-	1	0.46	0.45	18	3.0E-3	-2.53	0.633	1.0E-2	-
ptn25	1.7E-13	-12.78	0.10	7	0.52	0.6	72	1.1E-3	-2.96	0.633	5.5E-3	-
ptn26	2.2E-13	-12.66	-	1	0.97	0.84	114	9.6E-4	-3.02	0.633	3.1E-3	-
tsw31	8.1E-13	-12.09	-	-	2.17	2.37	140	1.1E-3	-2.96	0.633	5.0E-3	-
tsw32	7.1E-13	-12.15	0.66	31	1.12	1.09	842	1.4E-3	-2.86	0.633	8.3E-3	-
tsw33	7.8E-13	-12.11	0.61	27	0.81	1.03	1329	1.6E-3	-2.80	0.633	5.8E-3	-
tsw34	3.3E-13	-12.48	0.47	180	4.32	3.42	10646	6.7E-4	-3.18	0.633	8.5E-3	2.50E-03
alternate tsw34	1.5E-13	-12.81	0.75	180								
tsw35	9.1E-13	-12.04	0.54	31	3.16	-	595	1.0E-3	-2.99	0.633	9.6E-3	-
tsw3[67]	1.3E-12	-11.87	0.28	19	4.02	-	526	1.1E-3	-2.96	0.633	1.3E-2	-
tsw38	8.1E-13	-12.09	-	-	4.36	-	37	8.9E-4	-3.05	0.633	1.1E-2	-
tsw39	8.1E-13	-12.09	-	-	0.96	-	46	1.5E-3	-2.82	0.633	4.3E-3	-
ch1Ze	2.5E-14	-13.60	-	-	0.04	-	3	1.4E-3	-2.86	0.633	1.6E-4	-
ch1VI	2.2E-13	-12.66	-	-	0.10	-	11	2.1E-3	-2.69	0.633	6.1E-4	-
ch[23456]VI	2.2E-13	-12.66	-	-	0.14	-	25	1.9E-3	-2.73	0.633	7.7E-4	-
ch[2345]Ze	2.5E-14	-13.60	-	1	0.14	-	25	8.9E-4	-3.05	0.633	3.7E-4	-
ch6	2.5E-14	-13.60	-	-	0.04	-	-	1.4E-3	-2.86	0.633	1.6E-4	-
pp4	2.5E-14	-13.60	-	-	0.14	-	-	8.9E-4	-3.05	0.633	3.7E-4	-
pp3	2.2E-13	-12.66	-	-	0.20	-	-	1.6E-3	-2.78	0.633	9.7E-4	-
pp2	2.2E-13	-12.66	-	-	0.20	-	-	1.6E-3	-2.78	0.633	9.7E-4	-
pp1	2.5E-14	-13.60	-	-	0.14	-	-	8.9E-4	-3.05	0.633	3.7E-4	-
bf3	2.2E-13	-12.66	-	-	0.20	-	-	1.6E-3	-2.78	0.633	9.7E-4	-
bf2	2.5E-14	-13.60	-	-	0.14	-	-	8.9E-4	-3.05	0.633	3.7E-4	-
tr3	2.2E-13	-12.66	-	-	0.20	-	-	1.6E-3	-2.78	0.633	9.7E-4	-
tr2	2.5E-14	-13.60	-	-	0.14	-	-	8.9E-4	-3.05	0.633	3.7E-4	-
tcwf	2.7E-11	-10.57	-	-	1.90	-	-	3.8E-3	-2.42	0.633	2.9E-2	-
ptnf	3.1E-12	-11.51	-	-	0.54	-	-	2.8E-3	-2.55	0.633	1.1E-2	-
tcwf	1.5E-11	-10.82	-	-	1.70	-	-	3.2E-4	-2.49	0.633	2.5E-2	-
chnf	3.7E-13	-12.43	-	-	0.13	-	-	2.3E-3	-2.64	0.633	1.0E-3	-

DTNs: LB0205REVUZPRP.001 [159525]; LB0207REVUZPRP.001 [159526]

NOTE: k is permeability.
$_G$ refers to geometric mean.
σ is standard deviation.
N is number of samples.
f is fracture frequency.
α and m are fitting parameters for the van Genuchten water potential relationship.
Std refers to standard deviation for fracture porosity.

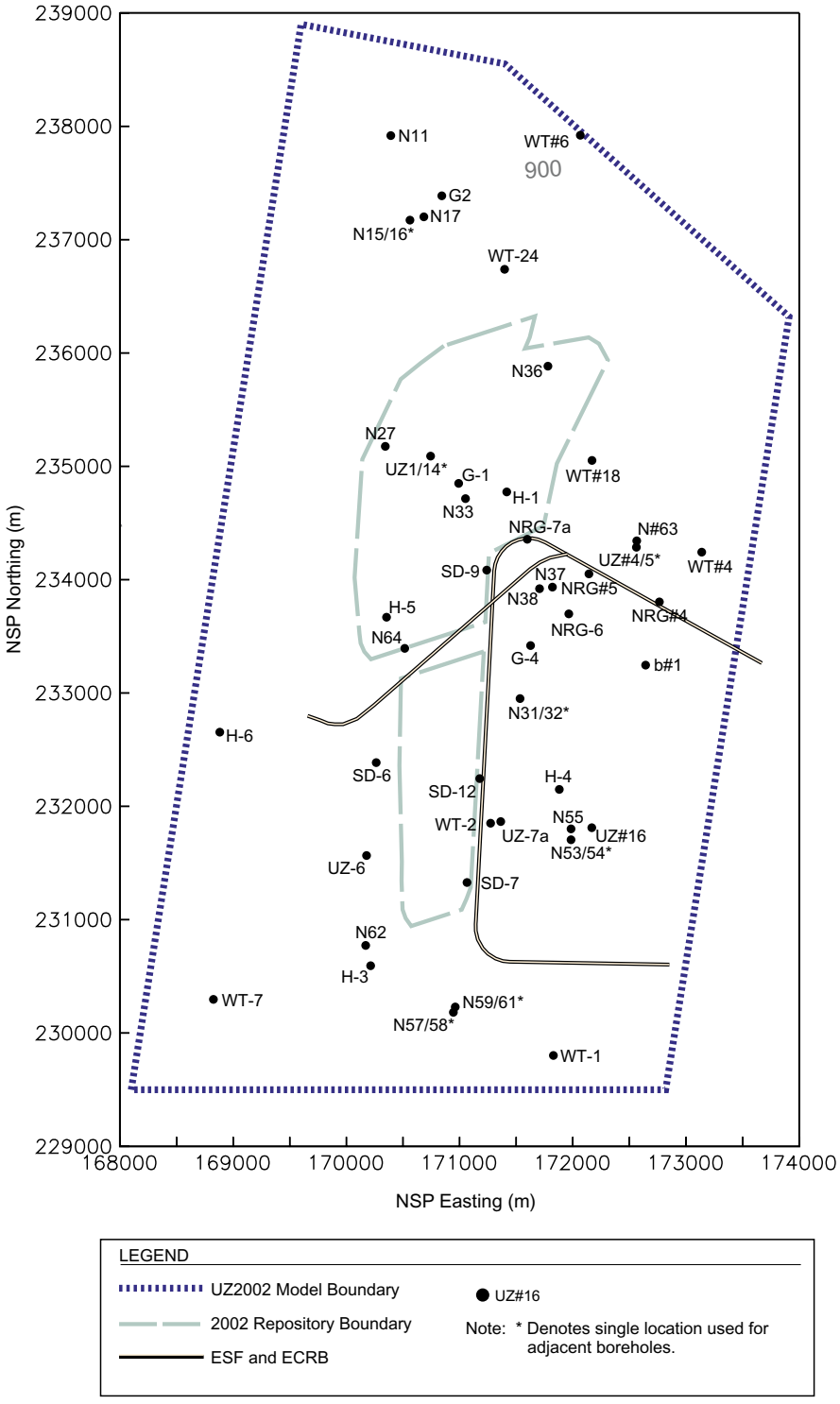

Source: BSC (2003 [160109], Figure 1b).

NOTE: NSP Refers to Nevada State Plane

Figure 1. Locations of Boreholes

4.1.2.2 Water-Potential Data

Water-potential data measured *in situ* in boreholes USW NRG-6, USW NRG-7a, UE-25 UZ#4, and USW SD-12 are used in the 1-D inversions and model validations. These boreholes do not intersect mapped faults, and thus the water-potential data are representative of the rock mass of Yucca Mountain. Water-potential data measured *in situ* in borehole USW UZ-7a are used for the 2-D inversions. This borehole intersects the Ghost Dance fault, and thus the water-potential data are judged to be representative of the faulted rock of Yucca Mountain. Water potential data measured *in situ* in borehole UE-25 UZ#5 are not used because this borehole is very close to borehole UE-25 UZ#4, such that the spatial representativeness of the inversion results could be distorted if both were included.

Water-potential data measured on core are not used because drying during drilling and/or handling may have substantially changed the water potential. In contrast with saturation data, for which the amount of change may be estimated (see Section 6.2.2), there is no way to reliably estimate the change in water potential. Such an estimate would depend on both the amount of saturation change and the relationship between saturation and water potential, and the uncertainty would be too great to contribute meaningful information to the parameter estimation procedure.

4.1.2.3 Pneumatic Pressure Data

Pneumatic pressure data measured *in situ* in boreholes UE-25 NRG#5, USW NRG-6, USW NRG-7a, USW SD-7, and USW SD-12 are used in the 1-D inversion and/or model validation. These boreholes do not intersect mapped faults, and thus the pneumatic pressure data from these boreholes are representative of the rock mass of Yucca Mountain. Pneumatic pressure data measured *in situ* in borehole USW UZ-7a are used in the 2-D inversion. This borehole intersects the Ghost Dance fault, and thus the pneumatic pressure data from this borehole are judged to be representative of the faulted rock of Yucca Mountain.

Pneumatic pressure data from boreholes UE-25 UZ#4 and UE-25 UZ#5 are not used for the 1-D inversion because they are close to a small, unnamed fault which, while it does not affect the *in situ* water-potential data, could affect the pneumatic data. While data from these boreholes and from USW NRG-6 do show the influence of the ESF, which is transmitted via faults, they are not used for calibration of fault parameters because three-dimensional (3-D) models would be required, and only a single parameter, Topopah Spring welded hydrogeologic unit (TSw) horizontal fracture permeability, could be calibrated.

4.1.2.4 Use of Established Fact Data

Established fact data are used in Equations 5 through 7 (Section 6.2.2). These data include physical properties of air, the molecular weight and critical temperature and critical pressure of both air and water, and mole fraction of water vapor in air. The data values and sources are specified in Section 6.2.2 of this report.

4.2 CRITERIA

The U.S. Nuclear Regulatory Commission (NRC) standard for a proposed repository at Yucca Mountain (10 CFR 63) provides the primary criteria for the development of this Model Report. Therein, Section 63.114 (a) requires that performance assessment include data related to the hydrology of Yucca Mountain, and Section 63.114 (b) requires that these data account for uncertainties and variabilities in parameter values. These requirements are expressed in Requirement PRD-002/T-015 of the *Project Requirements Document* (Curry and Loros 2002 [157916]). Section 63.304(4) requires that PA consider the full range of defensible and reasonable parameter distributions and not only extreme parameter values, and this requirement is expressed in Requirement PRD-002/T-025 of the *Project Requirements Document* (Curry and Loros 2002 [157916]).

The Acceptance Criteria against which this Model report will be judged to have met these requirements are given in *Yucca Mountain Review Plan, Draft Report for Comment* (NRC 2002 [158449]), Section 4.2.1.3.6 Flow Paths in the UZ, in section 4.2.1.3.6.3, AC 2: Data are sufficient for model justification (bullet 1: hydrological and thermal-mechanical-chemical values used in the safety case are adequately justified. Adequate descriptions of how the data were used, interpreted, and appropriately synthesized into the parameters are provided; bullet 5: sensitivity or uncertainty analyses are performed to assess data sufficiency, and determine the possible need for additional data; and bullet 6: Accepted and well documented procedures are used to construct and calibrate numerical models) and AC 3: Data uncertainty is characterized and propagated through the model abstraction (bullet 1: Models use parameter values, assumed ranges, probability distributions, and/or bounding assumptions that are technically defensible and reasonably account for uncertainties and variabilities; and bullet 6: Uncertainties in the characteristics of the natural systems and engineered materials are considered). The identified bullets from these ACs are addressed in Sections 6.2, 6.4, and 7 of this Model Report.

Values and uncertainties of hydrologic properties that are determined by the Calibrated Properties Model also affect calculation of seepage in that these values and uncertainties are used by the UZ Flow Model to provide boundary conditions for the seepage models. Therefore these additional ACs defined in section (NRC 2002 [158449]), 4.2.1.3.3 Quantity and Chemistry of Water Contacting Waste Packages and Waste Forms also apply. They are, in Section 4.2.1.3.3.3, AC 2: Data are sufficient for model justification (bullet 1: Geological, hydrological, and geochemical values used in the safety case are adequately justified. Adequate description of how the data were used, interpreted, and appropriately synthesized into the parameters is provided) and AC 3: Data uncertainty is characterized and propagated through the model abstraction (bullet 1: Models use parameter values, assumed ranges, probability distributions, and/or bounding assumptions that are technically defensible and reasonably account for uncertainties and variabilities). These ACs are addressed in Sections 6.2, 6.3, 6.4, and 7 of this Model Report.

4.3 CODES AND STANDARDS

No specific formally established standards have been identified as applying to this modeling activity.

INTENTIONALLY LEFT BLANK

5. ASSUMPTIONS

The assumptions documented below are necessary to develop the Calibrated Properties Model. This section presents the rationale for these assumptions and references the section of this Model Report in which each assumption is used. Other assumptions basic to the UZ Flow and Transport Model (UZ Model) of Yucca Mountain are elements of the conceptual model, which are summarized at the beginning of Section 6 and are fully documented in an Analysis/Model Report (AMR) entitled *Conceptual and Numerical Models for UZ Flow and Transport* (CRWMS M&O 2000 [141187]).

The following assumptions are used to develop the Calibrated Properties Model.

1. It is assumed that layers bf3 and bf2 have the same hydraulic properties as tr3 and tr2, respectively (Section 6.3.2).

No data except geologic contacts exist for layers tr3 or tr2 (the Tram Tuff). Because the Tram Tuff has a structure similar to the Bullfrog Tuff and the two tuffs are divided into similar model layers (BSC 2002 [159124], Table 4), the hydrologic properties should also be similar. Further, model layers tr3 and tr2 constitute only a small portion of the UZ in the northern part of the model area and along the foot wall of the Solitario Canyon fault, so the properties are not likely to have a large impact on simulations of flow and transport.

2. It is assumed that reported saturation values greater than 1.0 are equal to 1.0 (Section 6.2.2).

Measurement error causes calculated saturation values (based on measurements of initial, saturated, and dry weight) to be greater than 1.0, but this is not physically possible. Saturation is constrained to a maximum of 1.0.

Based on the rationales stated below each assumption, these assumptions do not need further confirmation.

INTENTIONALLY LEFT BLANK

6. MODEL DISCUSSION

The UZ Model is used to represent past, present, and future thermal-hydrological (TH) and chemical conditions within the UZ of Yucca Mountain. The UZ Model consists of hydrological (flow and transport) and thermal properties and a numerical grid, which together form input for the TOUGH family of simulators. This Model Report documents the development of some of the hydrologic properties for the UZ Model. Assumptions used in this section and their bases are presented in Section 5. The intended use of the output data developed using approaches in this section is given in Section 1.

The key scientific notebooks (with relevant page numbers) used for the modeling activities described in this Model Report are listed in Table 5.

Table 5. Scientific Notebooks

LBNL Scientific Notebook ID	M&O Scientific Notebook ID	Relevant Pages	Citation
YMP-LBNL-UZ-CFA-1	SN-LBNL-SCI-003-V2	84–97	Wang 2002 [160401]
YMP-LBNL-GSB-LHH-3	SN-LBNL-SCI-215-V1	65–98, 100	Wang 2002 [160401]
YMP-LBNL-GSB-LP-6	SN-LBNL-SCI-299-V1	9–21	Wang 2002 [160401]
YMP-LBNL-YSW-3	SN-LBNL-SCI-199-V1	98–99, 104	Wang 2002 [160401]

6.1 CONCEPTUAL MODEL, ALTERNATIVE MODELS, AND NUMERICAL SIMULATOR

Calibration of the UZ Model is a key step in its development. Calibration is necessary to refine the property estimates derived from laboratory and field data, so that they are suitable for use in the UZ Model and so that the UZ Model accurately depicts hydrological conditions in the mountain. The UZ Model considers large-scale hydrological processes; where properties are scale-dependent, upscaling will inherently be part of the calibration process. The calibration process also reduces property-estimate uncertainty and bias. Property estimates from laboratory and field data, like any other estimates, will have uncertainty associated with them because of data limitations (e.g., sampling and measurement biases, limited number of samples). The conceptual model and numerical schemes used to develop the numerical representation of the UZ Model have been documented in an AMR entitled *Conceptual and Numerical Models for UZ Flow and Transport* (CRWMS M&O 2000 [141187]). The aspects of the conceptual model and numerical schemes that are most relevant to this study are highlighted in this section. Alternative models and numerical approaches are also discussed in this section.

A variety of numerical approaches have been proposed to deal with flow and transport processes in fractured media at field scale (CRWMS M&O 2000 [141187], Section 6.4.1). When classified according to the manner in which fracture networks are treated in the model structure, the approaches fall into three groups: (1) continuum approaches (including effective continuum, dual continuum, and multiple interacting continua), (2) discrete fracture-network approaches, and (3) other approaches (e.g., a combination of the continuum approaches and the discrete fracture-

network approaches). Based on overall flow and transport behavior in the UZ, scale of the problem under consideration, and a compromise between modeling accuracy and computational feasibility, the dual-permeability method (a continuum approach) is considered appropriate for describing flow and transport in the UZ (CRWMS M&O 2000 [141187], Section 6.4.2). Consequently, the dual-permeability method is used for all the modeling studies documented in this report. The alternative approaches (including discrete fracture-network approaches and other approaches) generally involve computational generation of synthetic fracture networks and subsequent modeling of flow and transport in each individual fracture. While these approaches are useful as tools for concept evaluation, they are not practically feasible for dealing with large-scale problems (CRWMS M&O 2000 [141187], Section 6.4).

Because the PTn unit greatly attenuates episodic infiltration pulses, liquid water flow is considered to be approximately in steady state under ambient conditions (CRWMS M&O 2000 [141187], Sections 6.1.2 and 6.1.6). Steady-state liquid flow conditions are thus used in all the modeling studies documented in this report. Note that episodic flow through the PTn (possibly through faults) exists as indicated by the finding of "bomb-pulse" signature of ^{36}Cl in the UZ. However, this flow component is believed to carry only a small amount of water (CRWMS M&O 2000 [141187], Sections 6.1.6 and 6.1.7).

Heterogeneities exist at different scales within both the fracture and matrix continua in the UZ at Yucca Mountain. Treatment of subsurface heterogeneity and parameterization (use of a number of parameters to represent the heterogeneous distribution) is highly relevant to calibration of hydraulic properties. A geologic-based, deterministic approach is mainly used for characterizing subsurface heterogeneity in the UZ (CRWMS M&O 2000 [141187], Section 6.4.3). This is based on the following considerations: (1) overall behavior of large-scale flow and transport processes are mainly determined by relatively large-scale heterogeneities associated with the geologic structures of the mountain, (2) the heterogeneity model needs to be consistent with the availability of data, and (3) this approach is also supported by field observation (e.g., matrix-saturation distributions) (CRWMS M&O 2000 [141187], Section 6.4.3). Therefore, the heterogeneity of hydrological properties in this study is treated as a function of geologic layering, shown in Table 6, so that any one geologic layer has homogeneous properties (referred to as layer average properties), except where faulting or variable alteration (e.g., zeolitization) is present. In these cases, two sets of properties are used for layers with variable alteration, one for the portion of the layer that is altered beyond some threshold and one for the remaining portion. The Scientific Analysis report *Development of Numerical Grids for UZ Flow and Transport Modeling* (BSC 2003 [160109], Section 6) documents this process. Heterogeneity in faults is treated as a function of major hydrogeologic units (HGU), shown in Table 6, with the CHn and CFu combined (i.e., only four sets of hydrological properties are used for the faults).

The van Genuchten (1980 [100610], pp. 892–893) relations, originally developed for porous media, have been used as constitutive relationships for liquid flow in the UZ (CRWMS M&O 2000 [141187], Section 6.4.4). This treatment results from the use of porous-medium equivalence for describing flow in fractures. Recently, Liu and Bodvarsson (2001 [160110]) developed a new constitutive-relationship model for unsaturated flow in fracture networks, based mainly on numerical experiments. They found that the van Genuchten model is approximately valid for low fracture saturations corresponding to ambient conditions. Therefore, the van

Genuchten model is still used in this study. Note that model calibrations are performed using data collected under ambient conditions.

The base-case output data of the Calibrated Properties Model are developed from base-case, present-day infiltration maps (Section 6.2.5). However, to capture potential uncertainties introduced by the estimation of infiltration rates, alternative models based on the lower- and upper-bound infiltration maps are also fully developed and calibrated in this report (Section 6.2.5).

In a number of laboratory scale experiments, Glass et al. (1996 [139237]) demonstrated that gravity-driven fingering flow is a common flow mechanism in individual fractures. Fingering flow can occur at different scales. It has been well known in the subsurface hydrology community that flow and transport processes and the related parameters are scale-dependent (e.g., Neuman 1994 [105731]). Fingering flow at a fracture network scale, resulting from subsurface heterogeneity and nonlinearity involved in an unsaturated system, is a more important mechanism for liquid flow in the UZ than fingering flow in individual fractures. This is because the UZ flow model deals with flow and transport at large scales consisting of a great number of fractures. The active fracture model of Liu et al. (1998 [105729]) is used for considering the mechanism of fingering flow at a fracture network scale (CRWMS M&O 2000 [141187], Section 6.4.5). The active fracture concept is based on the reasoning that, as a result of fingering flow, only a portion of fractures in a connected, unsaturated fracture network contributes to liquid water flow. A detailed evaluation of the active fracture model based on both theoretical arguments and field observations will be presented in a Model Report describing analyses of hydrologic properties data.

Liquid flow occurs predominantly in the matrix in the PTn (see Table 6) and occurs only in the matrix in vitric portions of the CHn. In all other layers, liquid flow occurs predominantly in the fractures. The dominant matrix flow results from relatively high matrix permeabilities and low fracture densities in these units (CRWMS M&O 2000 [141187], Section 6.1.2). This conceptual model is supported by UZ flow tests conducted in nonwelded tuffs at Busted Butte and in the Exploratory Studies Facility (ESF) Alcove 4. The tests at Busted Butte conducted in the upper CHn(v) show that flow took place in the matrix; fracture flow was not observed, given the limits of the observational capability (even though fractures are present) (BSC 2001 [160828], Section 6.8.9). Tests in ESF Alcove 4 conducted in the PTn unit also show that flow around a large, through-going fracture is matrix-dominant (BSC 2001 [158463], Section 6.7).

It is well known that permeability is scale-dependent (Neuman 1994 [105731]). Calibrated properties are necessary on two scales, mountain-scale and drift-scale. Calibration of the mountain-scale properties considers pneumatic pressure data that reflect the mountain-scale process of barometric pumping. Mountain-scale properties are intended for use in models of processes at the mountain scale. Calibration of the drift-scale properties does not consider the pneumatic pressure data. Drift-scale properties are intended for use in models of processes at the drift scale.

In this study, iTOUGH2 V5.0 (LBNL 2002 [160106]) is used for model calibration. This program uses the integral-finite-difference method for spatial discretization, and is a general-purpose inverse and forward numerical simulator for multidimensional, coupled fluid and heat

flow of multiphase, multicomponent fluid mixtures in porous and fractured media. To the best of YMP investigators' knowledge, iTOUGH2 represents the state of the art in the area of inverse modeling of multiphase flow process in fractured media. This code has been comprehensively tested under different conditions (Finsterle 1998 [103783]; 1999 [104367]). In an inversion, iTOUGH2 V5.0 (LBNL 2002 [160106]) evaluates the goodness of calibration fit using a least-squares approach that minimizes the sum of the squared weighted residuals (objective function), while the weighting factor is the inverse of the uncertainty data. The objective function, F, is expressed as (Finsterle 1999 [104367], Section 2.6.4):

$$F = \sum_i \frac{(z_i * - z_i)^2}{U_i^2} \qquad \text{(Eq. 1)}$$

where z_i* and z_i are measurement i and the corresponding simulation result, respectively. U_i is the uncertainty of measurement z_i*. iTOUGH2 V5.0 (LBNL 2002 [160106]) simulates fluid flow by numerically solving the following governing equation (for an arbitrary flow domain V_n with the boundary Γ_n) (Pruess 1987 [100684], Section 3):

$$\frac{d}{dt}\int_{V_n} M dV = \int_{\Gamma_n} F \bullet n d\Gamma + \int_{V_n} q dV \qquad \text{(Eq.2)}$$

where t is time, M is the accumulation (storage) term, F is the mass flux, n is the unit vector normal to the domain boundary, and q is the source term.

The upstream weighting numerical technique for the relative permeability is used for inversions. While this is considered to be an approximation for calculating flow from fractures to the matrix (matrix imbibition), it is still expected to be a reasonable scheme for this study. First, it is well known that upstream weighting is a robust approach to avoid numerical oscillations for multiphase flow in highly heterogeneous systems (Forsyth et al.1995 [161743]). Simulation of unsaturated flow in the UZ is numerically challenging because of a combination of heterogeneity and nonlinearity. To perform numerical simulation for such a complex system, both numerical accuracy and computational feasibility need to be considered. It is a practically reasonable choice to use this scheme to avoid the potential numerical problems. Second, use of the approach is not expected to result in significant errors for simulating matrix imbibition processes in the UZ. In nonwelded units, the flow mainly occurs in the matrix, and the flow component from fractures to the matrix is expected to be small. In the welded units, flow mainly occurs in fractures (because of small matrix permeability), again resulting in a relatively small flow component from fractures to the matrix. Finally, the approximation introduced by the weighting scheme is also compensated by the model calibration procedure that includes the effects of both numerical grids and numerical schemes.

Table 6. GFM2000 Lithostratigraphy, UZ Model Layer, and Hydrogeologic Unit Correlation

Major Unit (Modified from Montazer and Wilson 1984 [100161])	**GFM2000 Lithostratigraphic Nomenclature***	**UZ Model Layer**	**Hydrogeologic Unit (Flint 1998 [100033], Table 1)**
Tiva Canyon welded (TCw)	Tpcr	tcw11	CCR, CUC
	Tpcp	tcw12	CUL, CW
	TpcLD		
	Tpcpv3	tcw13	CMW
	Tpcpv2		
Paintbrush nonwelded (PTn)	Tpcpv1	ptn21	CNW
	Tpbt4	ptn22	BT4
	Tpy (Yucca)		
		ptn23	TPY
		ptn24	BT3
	Tpbt3		
	Tpp (Pah)	ptn25	TPP
	Tpbt2	ptn26	BT2
	Tptrv3		
	Tptrv2		
Topopah Spring welded (TSw)	Tptrv1	tsw31	TC
	Tptrn		
		tsw32	TR
	Tptrl, Tptf	tsw33	TUL
	Tptpul, RHHtop		
	Tptpmn	tsw34	TMN
	Tptpll	tsw35	TLL
	Tptpln	tsw36	TM2 (upper 2/3 of Tptpln)
		tsw37	TM1 (lower 1/3 of Tptpln)
	Tptpv3	tsw38	PV3
	Tptpv2	tsw39 (vit, zeo)	PV2

Source: BSC (2003 [160109], Table 11).

Table 6. GFM2000 Lithostratigraphy, UZ Model Layer, and Hydrogeologic Unit Correlation (cont.)

Major Unit (Modified from Montazer and Wilson 1984 [100161])	GFM2000 Lithostratigraphic Nomenclature*	UZ Model Layer	Hydrogeologic Unit (Flint 1998 [100033], Table 1)
Calico Hills nonwelded (CHn)	Tptpv1	ch1 (vit, zeo)	BT1 or BT1*a* (altered)
	Tpbt1		
	Tac (Calico)	ch2 (vit, zeo)	CHV (vitric) or CHZ (zeolitic)
		ch3 (vit, zeo)	
		ch4 (vit, zeo)	
		ch5 (vit, zeo)	
	Tacbt (Calicobt)	ch6 (vit, zeo)	BT
	Tcpuv (Prowuv)	pp4	PP4 (zeolitic)
	Tcpuc (Prowuc)	pp3	PP3 (devitrified)
	Tcpmd (Prowmd)	pp2	PP2 (devitrified)
	Tcplc (Prowlc)		
	Tcplv (Prowlv)	pp1	PP1 (zeolitic)
	Tcpbt (Prowbt)		
	Tcbuv (Bullfroguv)		
Crater Flat undifferentiated (CFu)	Tcbuc (Bullfroguc)	bf3	BF3 (welded)
	Tcbmd (Bullfrogmd)		
	Tcblc (Bullfroglc)		
	Tcblv (Bullfroglv)	bf2	BF2 (nonwelded)
	Tcbbt (Bullfrogbt)		
	Tctuv (Tramuv)		
	Tctuc (Tramuc)	tr3	Not Available
	Tctmd (Trammd)		
	Tctlc (Tramlc)		
	Tctlv (Tramlv)	tr2	Not Available
	Tctbt (Trambt) and below		

Source: BSC (2003 [160109], Table 11).

6.2 MODEL INPUTS

This section discusses model inputs for parameter calibration activities documented in this report. These inputs include numerical grids, infiltration rates, matrix-saturation and water-potential data, pneumatic pressure data and rock-hydraulic-property data. Some model inputs for fault property calibration are documented in Section 6.3.4.

6.2.1 Numerical Grids

One-dimensional, vertical-column numerical grids and a two-dimensional, cross-sectional numerical grid are used for the corresponding model calibrations. Numerical grids under DTN: LB02081DKMGRID.001 [160108] are slightly modified in this study (Wang 2002 [160401], SN-LBNL-SCI-003-V2, pp. 85–86). The eight-character element-name format in this DTN is not compatible with all necessary iTOUGH2 V5.0 (LBNL 2002 [160106]) features. In response, the element names are converted to a five-character format. In an eight-character name, the first character is either “F” or “M” (corresponding to fracture or matrix element). The second and

third characters are simply zeros. The fourth and fifth characters represent grid layers and the corresponding material layers. The last three characters are the name of the corresponding column. In the corresponding five-character name, the first character is again "F" or "M". The second character (0, A, B, …Z) represents grid layers within given material (model) layers defined in Table 6. The third character (1, 2, …9, A, B, … Z) is an indicator of the material layer. The last two characters represent names of the corresponding columns. To be consistent with the conceptual model regarding water flow in nonwelded vitric units (Section 6.1), investigators effectively remove fractures in vitric regions by reducing (by 50 orders of magnitude) the connection areas between fracture elements in these units and the corresponding matrix elements. Connections are also added between fractures in welded layers and matrix in nonwelded layers, to facilitate flow between matrix and fractures at interfaces where the fracture frequency changes significantly.

6.2.2 Matrix-Saturation and Water-Potential Data

Saturation and water-potential data, which are inverted to obtain the calibrated parameter sets, are developed so that they can be compared to the numerical model predictions. The core saturation data are available on intervals as small as 0.3 m. To compare these data to the saturation profiles predicted by the numerical model on intervals as large as several tens of meters (corresponding to model layer thickness), investigators averaged the data. The averaged data and their uncertainties are used for calibrating UZ parameters (Section 6.3). *In situ* water-potential data are measured at depth intervals equal to or greater than the numerical grid spacing, so these data do not need to be averaged. The *in situ* water-potential data do need to be analyzed, however, as discussed below, to determine when the sensor is in equilibrium with the surrounding rock. Inversions using iTOUGH2 V5.0 (LBNL 2002 [160106]) need both averaged (gridblock scale) matrix saturation and water-potential data and their uncertainties as inputs. The procedures to determine these data values and their uncertainties are also described below.

Saturation Data from Core (DTNs: MO0109HYMXPROP.001 [155989]; GS980808312242.014 [106748]; GS980708312242.010 [106752])—The number, arithmetic mean, and standard deviation of the core measurements (see Section 4.1.2.1 for description of data) that correspond to the intervals covered by each numerical grid element are calculated using software aversp_1 V1.0 (LBNL 2002 [146533]). The elevations of core sample locations are determined from borehole collar elevations from file contracts00md.dat in DTN: MO0012MWDGFM02.002 [153777] and the depth of the top of the Tptrn from DTN: GS940208314211.008 [145581] for borehole USW UZ-N57, N59 and N61 (Wang 2002 [160401], SN-LBL-SCI-003-V2, p. 84). Values greater than 1.0 are assumed to be 1.0 (Assumption 2, in Section 5).

iTOUGH2 V5.0 (LBNL 2002 [160106]) allows the data to be weighted. The weight of each saturation data point is estimated from the number of measurements, the standard deviation of the measurements, and estimates of handling and measurement error. The total error, *TE*, which is equal to the inverse of the weight, is

$$TE = SE + ME + HE \quad \text{(Eq. 3)}$$

where *SE* is the standard error, *ME* is the measurement error, and *HE* is the handling error. Standard error, *SE*, is defined here as

$$SE = \frac{\sigma}{\sqrt{N}} \quad \text{(Eq. 4)}$$

where σ is the unbiased estimate of the standard deviation and *N* is the number of measurements. If there is no estimate of the standard deviation because of N=1, σ and thus *SE* are set to 0.05, within the range of estimated SE values for N>1. Flint (1998 [100033], p. 17) reports that the measurement error for bulk properties is less than 0.5%. The measurement error for saturation is thus taken to be 0.005.

Drying of core during handling is a potential source of error for saturation data (Flint 1998 [100033], pp. 18–19; Rousseau et al. 1999 [102097], pp. 129–131). The HE is estimated for the core drying effects. Saturation is not easily quantifiable because of the variable nature of the forces controlling the drying. Drying during handling at the surface is related to saturation, water potential (and variation of water potential with saturation), and temperature of the core—as well as temperature, pressure, relative humidity, and speed of the air around the core. Drying of the core during drilling is related to similar factors. Rather than correct the measured saturation data by an uncertain drying estimate, a contribution to the total uncertainty of the saturation data is made by an estimate of drying losses. This contribution is included as the handling error, *HE*, in Equation 3 above.

A simplified model of core drying during handling is used to estimate the rate of evaporation from the core. A fully saturated core is approximated as a spherical rock with a surface that is always completely wet and that has the same area as the core. A solution for evaporation from a spherical drop of water in an air stream is given by Bird et al. (1960 [103524], p. 648) as

$$W = \eta \pi \delta^2 \frac{x_0 - x_\infty}{1 - x_\infty} \quad \text{(Eq. 5)}$$

where *W* is the evaporation rate, η is the mass-transfer coefficient of water vapor in air, δ is the diameter of a sphere with the same surface area as the core, x_0 is the water mole fraction in the air at the surface of the core, and x_∞ is the water mole fraction in air far away from the core. The mass-transfer coefficient of water vapor in air, η, is given by Bird et al. (1960 [103524], p. 649) as

$$\eta = \frac{cD}{\delta}\left[2 + 0.6\left(\frac{v\delta\rho}{\mu}\right)^{1/2}\left(\frac{\mu}{D\rho}\right)^{1/3}\right] \quad \text{(Eq. 6)}$$

where *c* is the total molar concentration of the air-water mixture, *D* is the effective binary diffusivity of water vapor in air, *v* is air speed, ρ is density of air, and μ is viscosity of air.

Effective binary diffusivity, D [cm^2/s], for an air and water-vapor (components A and B) mixture is given by Bird et al. (1960 [103524], p. 505) as

$$D = \frac{3.64\times10^{-4}}{p}\left(\frac{T}{\sqrt{T_{cA}T_{cB}}}\right)^{2.334}(p_{cA}p_{cB})^{1/3}(T_{cA}T_{cB})^{5/12}\left(\frac{1}{M_A}+\frac{1}{M_B}\right)^{1/2} \qquad \text{(Eq. 7)}$$

where p is pressure (atm), T is temperature (K), and p_c, T_c, and M are the critical pressure (atm), critical temperature (K), and molecular weight (g/g-mole), respectively, of components A and B.

The evaporation rate is estimated by setting the temperature of the core at 25°C and the temperature, pressure, relative humidity, and speed of the air far from the core at 30°C, 1 atm, 25%, and 3 km/h, respectively. These are all reasonable values for field conditions at Yucca Mountain. Neglecting the small effect of the water vapor in the air, the physical properties of air at 27.5°C (the average temperature) are $c = 4.05 \times 10^{-5}$ g-mole/cm^3, $\rho = 0.00118$ g/cm^3, and $\mu = 1.84 \times 10^{-4}$ g/cm/s (Roberson and Crowe 1990 [124773], p. A-22). The molecular weight, critical temperature and critical pressure of air are 28.97 g/g-mole, 132 K, and 36.4 atm, respectively (Bird et al. 1960 [103524], p. 744). The molecular weight and critical temperature and pressure of water are 18.02 g/g-mole, 647.25 K, and 218.3 atm, respectively (Weast 1987 [114295], pp. B-94, F-66). The mole fraction of water vapor in air at the surface of the core, x_0, is 0.0313 (Weast 1987 [114295], p. D-190). Given a relative humidity of 25%, the mole fraction of water vapor in air far from the core, x_∞, is 0.0126 (Weast 1987 [114295], p. D-190). The core is approximately 7 cm in diameter and 10 cm in length (Flint 1998 [100033], p. 11). Using these values, an evaporation rate of 2.69×10^{-4} g-mole/s is calculated based on Equations 5–7.

At this evaporation rate, the saturation of a fully saturated core of matrix porosity 22.3% (a typical value for tuff matrix [Table 3]) will be reduced by 2.2% after 5 minutes, which is the handling time given by Flint (1998 [100033], p. 11). A fully dry core will have no reduction in saturation. Using these two points, a linear dependence of saturation change on saturation yields the relation

$$\Delta S = 0.022S \qquad \text{(Eq. 8)}$$

where S is the uncorrected saturation value and ΔS is saturation change resulting from handling, or HE. Although the actual relation between ΔS and S may be much more complex than Equation 8, this equation is in practice adequate for estimating HE here. Average porosity for the entire mountain is calculated as a layer-thickness weighted average of individual layer porosities. Calculations for handling, measurement and total errors in saturation data are performed with Excel file layavsat.xls (Attachment I). Also note that water lost to drilling air is not considered here, because an approach to accurately estimate water loss is not available. However, the estimation of handling errors does not consider the effect of matrix capillary pressure, resulting in overestimated handling errors. This may partially compensate for the effects of water lost to drilling air.

***In Situ* Water Potential Data—**Measuring water potential *in situ* requires that the rock near the borehole and the granular fill of the borehole come into equilibrium with the surrounding rock. Prior to installation of the *in situ* sensors, these boreholes were open, and rock immediately around the borehole may have dried out (Rousseau et al. 1999 [102097], pp. 143–151). Thus, the *in situ* data (see Section 4.1.2.2 for description of data) vary with time for given locations and need to be evaluated to determine the equilibrium value of the data.

Data are available from boreholes USW NRG-6 and USW NRG-7a from 11/94 through 3/98, from borehole UE-25 UZ#4 from 6/95 through 3/98, and from borehole USW SD-12 from 11/95 through 3/98 in the DTNs listed above in Section 4. Each DTN covers from three to six months of data. The arithmetic average and trend (i.e., slope) of the data points for the time period covered by each DTN for each borehole, depth, and instrument station (there are two instrument stations per depth) were calculated. Values for each instrument station were then compared between DTNs (providing an approximate time history of water potentials) to find the value that best represented the equilibrium value. The determined *in situ* water potential values are available from file in_situ_pcap2.xls in DTN: LB991091233129.001 [125868]. This file is used as a direct input into the Calibrated Properties Model (Section 6.3). This DTN was mainly developed from DTNs: GS950208312232.003 [105572], GS951108312232.008 [106756], GS960308312232.001 [105573], GS960808312232.004 [105974], GS970108312232.002 [105975], GS970808312232.005 [105978], GS971108312232.007 [105980], and GS980408312232.001 [105982].

Rousseau et al. (1999 [102097], p. 144) give ± 0.2 MPa as the 95% confidence interval (two standard deviations) for the *in situ* water-potential measurements. One standard deviation, 0.1 MPa, is used as an estimate for the uncertainty. Because water potential is lognormally distributed, the standard error of log(water potential), $SE_{\log(\Psi)}$, is estimated as

$$SE_{\log(\Psi)} = \log(\Psi + 0.1) - \log(\Psi) \quad \text{(Eq. 9)}$$

where Ψ is the value of the water potential data point in MPa. The calculation of the standard error is performed using Excel file in_situ_pcap.xls (Attachment I).

6.2.3 Pneumatic Pressure Data

Thirty days of data from each borehole (see Section 4.1.2.3 for description of data) are used for the inversions (and/or model validations). Several criteria are used to select data for the inversions: The data must include both diurnal pressure changes and longer-period, weather-associated pressure changes; and must have been obtained prior to any influence from construction of the ESF. Table 7 shows the starting and ending dates for the data that were used in the inversion. Data from the instrument station or port nearest the bottom of the TCw are included because they show the lack of attenuation and lag in the barometric signal through the TCw. Data from stations between the lowermost in the TCw and the surface are not included, because they would not add information to the inversion and would weight the TCw data more than other data. Data from all instrument stations or ports in the PTn are included because there is substantial attenuation and lag in the barometric pumping signal through the PTn. Individual layers in the PTn are expected to have widely variable permeability, so it is important to include

data that show the amount of barometric-signal attenuation and lag in different layers of the PTn. Data from the uppermost and lowermost instrument stations or ports in the TSw are included, because they show the lack of significant attenuation and lag in the barometric pumping signal characteristics through the TSw. Data from the stations in between the uppermost and lowermost stations are not included, for the same reason cited above for the TCw data. Table 7 shows the subunit in which the sensors are placed. Data from the two lowest instrument stations in borehole USW SD-12 are not included because these data are affected by the presence of perched water, which is not adequately reproduced in the 1-D simulations. Data from the third-lowest instrument station in USW SD-12 are not included because it was not properly isolated from the surface (Rousseau et al. 1997 [100178], p. 31). Data from USW NRG-6 are used for model validation only (Section 7) and therefore not included in Table 7. The elevation of a location where gas pressure was monitored is determined by the ground surface elevation of the corresponding boreholes (available from Contacts00md.dat of DTN: MO0012MWDGFM02.002 [153777]) minus depths of the measurement locations (available from DTNs in Table 7).

Table 7. Pneumatic Pressure Data Used for Inversion

Borehole	Subunit	Dates	Elevation (m)
UE-25 NRG#5	Tpcp	7/17–8/16/95	1211.3
	Tpy	7/17–8/16/95	1194.8
	Tpp	7/17–8/16/95	1177.1
	Tpbt2	7/17–8/16/95	1161.0
	Tptrn	7/17–8/16/95	1143.9
	Tptpmn	7/17–8/16/95	1008.3
USW NRG-7a	Tpcp	3/27–4/26/95	1276.8
	Tpy	3/27–4/26/95	1231.7
	Tptrn	3/27–4/26/95	1164.0
	Tptpul	3/27–4/26/95	1078.7
USW SD-7	Tpcp	4/5–5/5/96	1271.6
	Tpp	4/5–5/5/96	1256.4
	Tptrn	4/5–5/5/96	1241.4
	Tptpmn	4/5–5/5/96	1119.2
USW SD-12	Tpcp	12/1–12/31/95	1258.5
	Tpbt2	12/1–12/31/95	1232.0
	Tptrn	12/1–12/31/95	1217.1
	Tptpll	12/1–12/31/95	1001.3

DTNs: GS000608312261.001 [155891]; GS960808312232.004 [105974]; GS950208312232.003 [105572]; GS960908312261.004 [106784]; GS951108312232.008 [106756]; GS960308312232.001 [105573]: MO0012MWDGFM02.002 [153777]

6.2.4 Prior Information

Uncalibrated rock-property data (Tables 3 and 4) are used as prior information. These data are just as important to the parameter calibration as data on the state of the system (e.g., saturation). The combination of the two types of information allows the calibration to match the data as well as possible, while simultaneously estimating model parameters that are reasonable according to the prior information. Standard errors of parameters for weighting the prior information are taken from Tables 3 and 4. For matrix permeability, the weight is estimated as the inverse of the standard error given in Equation 4. Because permeability is lognormally distributed, σ and thus *SE* are estimated for the log-transformed permeabilities, i.e. log(k). The number of samples used for calculation of the standard error does not include nondetect samples (i.e., N in Equation 4 is the total number of samples minus the number of nondetect samples, as shown in Table 3). As discussed below, drift-scale fracture permeabilities are directly assigned from the prior information, and therefore standard error data are not needed for model calibration of drift-scale fracture permeabilities. Mountain-scale fracture permeabilities, however, are calibrated using the pneumatic data, because the pneumatic data correspond to a mountain-scale process. In inversions of pneumatic pressure data, prior information does not significantly contribute to the objective function (Section 6.3.1) because the number of data points is considerably larger than the number of calibrated fracture permeabilities. Therefore, for simplicity, a standard error of two orders of magnitude is assigned to fracture permeabilities in TCw and PTn for calibrating mountain-scale nonfault property sets, and a standard error of one order of magnitude for calibrating fault property sets. For layers tsw31 through tsw37, fracture permeabilities are calibrated by a technique that does not require weighting, so no standard errors are used (see Section 6.3.3). Standard error is given for log(α) because α is lognormally distributed. For fracture properties, the uncalibrated value of α_F is estimated based on fracture permeability and fracture frequency data (BSC 2001 [159725], Section 6). Since a directly measured α_F value is not available, a relatively large value of 2 (or two orders of magnitude, compared with values for matrix log(α)) is assigned as standard error for log(α_F) in inversions.

6.2.5 Boundary and Initial Conditions

Infiltration rates (DTN: GS000308311221.005 [147613]) are used as top boundary conditions during model calibration activities. The base-case present-day infiltration map and the lower- and upper-bound present-day infiltration maps are used to calculate infiltration rates corresponding to the calibration boreholes. For each infiltration map (DTN: GS000308311221.005 [147613]), the infiltration rate at each calibration borehole, shown in Table 8, is determined, using infil2grid V1.6 (LBNL 1999 [134754]), as an averaged infiltration-rate value over a circular area of 200 m radius with the center at the borehole location (Wang 2002 [160401], SN-LBNL-SCI-215-V1, pp. 93–94; SN-LBNL-SCI-003-V2, p. 87). A relatively large value of the radius (compared with the lateral gridblock sizes) is used because of capillary-dispersion considerations (lateral redistribution of moisture resulting from a capillary gradient from wet areas under high infiltration zones to dry areas under low infiltration zones) within the PTn unit. During fault-parameter calibration involving the 2-D numerical grid, the infiltration rates are directly calculated using infil2grid V1.7 (LBNL 2002 [154793]), based on the corresponding sizes of top elements of the grid. In all the simulations in this study, bottom boundaries correspond to the water table. Note that three different infiltration boundary conditions were used here for inversions, to examine alternative models and the corresponding

parameter sets. For inversions of matrix saturation and water potential data, steady-state water flow fields are simulated.

Table 8. Area-Averaged Infiltration Rates (mm/yr) Used in the 1-D Data Inversions

Borehole	Lower Bound	Base Case	Upper Bound
USW NRG-6	1.00E-4	0.53	2.72
USW SD-6	1.17	6.54	15.33
USW SD-7	1.11E-3	1.06	2.59
USW SD-9	0.08	1.04	3.63
USW SD-12	0.80	3.37	7.95
UE-25 UZ#4	0.02	0.41	3.79
USW UZ-14	0.20	2.28	8.72
UE-25 UZ#16	1.00E-4	0.22	2.91
USW UZ-N11	3.64	10.62	22.67
USW UZ-N31	0.54	1.75	4.45
USW UZ-N33	0.08	0.53	4.76
USW UZ-N37	1.00E-4	0.07	4.40
USW UZ-N53	1.00E-4	0.16	1.45
USW UZ-N57	0.23	5.03	18.08
USW UZ-N61	0.15	4.84	17.58
USW WT-24	1.87	5.50	11.96

Source: Wang 2002 [160401], SN-LBNL-215-V1, pp. 93–94

The time-varying pneumatic pressure boundary condition used to simulate barometric pumping is a combination of records from the surface at boreholes USW NRG-6 and USW NRG-7a. The record from USW NRG-7a is used as the basis for the surface signal. Where there are gaps in the data from USW NRG-7a, data from USW NRG-6 are used to fill them. Four discontinuous 60-day periods are concatenated into a 240 day record of barometric pressure. The four 60-day periods cover the four 30-day periods selected for data inversion and the 30 days immediately preceding each. The 30 days preceding the data sets are included in the simulations to develop a dynamic pressure history in the simulation. Because pressures are constantly changing in the real system, pneumatic pressure is never in equilibrium (i.e., pneumatically static conditions are never achieved). Initial conditions for pneumatic simulations are either pneumatically static conditions or dynamic conditions from a previous simulation. When the barometric signal is applied to the upper boundary of the model, the pressure variations within the model quickly equilibrate to the boundary condition, because propagation of the pressure fronts from the upper boundary is all that is necessary. The mean pressure, however, takes slightly longer to equilibrate, because flow from the upper boundary must reach the entire model. Previous work with the Yucca Mountain models have shown that after 30 days, the effects of the initial conditions are insignificant (i.e., dynamic pneumatic conditions corresponding to the current dynamic boundary conditions are developed) (Ahlers et al. 1998 [124842], p. 224). This is also true when the initial conditions are the dynamic conditions at the end of a 60-day period (i.e., when switching from one 60-day boundary condition period to the next). The mean pressure at the collar (surface) of each borehole is different because each borehole is at a different elevation. The main pressure of the pneumatic bounding condition for each boundary node is calculated based on the initial condition. The formatted gas pressure data (files with an extension txt) and top boundary condition (file timvsp.dat) from DTN: LB991091233129.001 [125868] are directly

used in the relevant modeling studies (Section 6.3). Observed pneumatic pressure data (input files) were taken at irregular time intervals. Therefore, iTOUGH2 V5.0 (LBNL 2002 [160106]) automatically interpolates the data to obtain a data set suitable for inversions. These interpolated data are plotted in Figures 8 and 11.

6.2.6 Other Considerations

Dominant fracture flow throughout the TSw is part of the current conceptual model (Section 6.1). To incorporate this conceptual model more easily, liquid-water fluxes reflecting 100% fracture flow in the TSw are used as an input in inversions for matrix-to-fracture connections between ptn26 and tsw31 and fracture to fracture connections between tsw31 and tsw32, tsw32 and tsw33, and tsw33 and tsw34 (Wang 2002 [160401], SN-LBNL-SCI-003-V2, p. 89). Note that this does not actually result in 100% fracture flux in simulated flow fields, although this does give the required dominant fracture flow throughout the TSw.

6.3 UZ FLOW MODEL PARAMETER CALIBRATION

6.3.1 General Calibration Approach

Inversion is an iterative process in which predictions from a numerical model are compared to data. The numerical model parameters are adjusted (calibrated) to improve the match between the model prediction and the data. Data that are inverted to provide the calibrated properties documented in this Model Report include saturation in the rock matrix, water potential in the rock matrix, and pneumatic pressure in the fractures. Hydrologic-property estimates from laboratory and field measurements, which provide initial estimates for model parameters, also are included as data in the inversion. These data, which are referred to as "prior information" in this report, are just as important to the inversion as data about the state of the system (e.g., saturation). The combination of the two types of information allows the inversion to match the data as well as possible, while simultaneously estimating model parameters that are reasonable according to the prior information. Three different kinds of parameter sets, drift-scale, mountain-scale and fault parameter sets, are determined from these calibration activities.

The software iTOUGH2 V5.0 (LBNL 2002 [160106]) is used to carry out the automatic portion of the inversion process. This software not only allows the consideration of both data and prior information, but also allows them to be weighted. The data and prior information are weighted according to the uncertainty of the estimated value. The software attempts to minimize the sum of the squared, weighted residuals (called the objective function). It does this by iteratively adjusting (calibrating) selected model parameters. Finsterle (1998 [103783]; 1999 [104367]) describes further details of the inversion approach. Also note that averaged matrix saturation values (for numerical gridblocks) (Section 6.2.2) are used in inversions. The averaged data are also plotted in Figures 2, 4, 6, and 9.

6.3.2 Calibration of Drift-Scale Parameters

Calibration procedure—One-dimensional inversion of the matrix-saturation and water-potential data is carried out for drift-scale parameters. The EOS9 module (Richards' equation) of iTOUGH2 V5.0 (LBNL 2002 [160106]) is used for the inversion. The one-dimensional

submodels correspond to 16 surface-based boreholes from which saturation and water potential have been measured. Table 9 shows the types of data used from each borehole, and Figure 1 shows the locations of some selected boreholes. Steady-state water flow is simulated simultaneously in all columns. Layer-averaged effective parameters are estimated, i.e., the same set of parameter values is used for each geologic layer in all columns.

Table 9. Data Used for 1-D Calibration of Drift-Scale Properties from Each Borehole

Borehole	Matrix Liquid Saturation (core)	Matrix Liquid Water Potential (*in situ*)
USW NRG-6		✔
USW SD-6	✔	
USW SD-7	✔	
USW SD-9	✔	
USW SD-12		✔
UE-25 UZ#4		✔
USW UZ-14	✔	
UE-25 UZ#16	✔	
USW UZ-N11	✔	
USW UZ-N31	✔	
USW UZ-N33	✔	
USW UZ-N37	✔	
USW UZ-N53	✔	
USW UZ-N57	✔	
USW UZ-N61	✔	
USW WT-24	✔	

DTNs: MO0109HYMXPROP.001 [155989]; GS980808312242.014 [106748]; GS980708312242.010 [106752]; LB991091233129.001 [125868].

Three calibrated parameter sets are produced, one for each present-day infiltration case (Section 6.2.5). The infiltration scenarios are key inputs to the UZ Model because flow and transport are dependent on the amount of water infiltrating into the mountain. The base-case infiltration scenario gives the expected, spatially varying infiltration rates over Yucca Mountain, and parameters calibrated using this scenario are the base-case parameter set. The upper- and lower-bound infiltration scenarios give bounds to the uncertainty of the base-case infiltration scenario. Parameters calibrated using the bounding scenarios are also provided. This gives the parameter sets that consider underestimation and overestimation of the present-day infiltration by the base-case scenario.

The one-dimensional drift-scale property calibration is documented in scientific notebooks by Wang (2002 [160401], SN-LBNL-SCI-215-V1, pp. 65–70, 100; SN-LBNL-SCI-003-V2, pp. 84–97).

Choice of Parameters for Calibration—Model parameters to be estimated are matrix permeability, k, matrix van Genuchten parameter α (van Genuchten 1980 [100610], pp. 892–

893), fracture van Genuchten parameters α and a active-fracture-model parameter, γ (Liu et al. 1998 [105729]). Other parameters are not changed in the calibration. These parameters are calibrated for model layers shown in Table 6 (except the zeolitic portion of CHn), though in some cases a common parameter value is estimated for groups of layers. (Details of which layers are grouped for parameter estimation are discussed below.) Inverse modeling involves many forward simulations and is therefore computationally intensive. One-dimensional columnar models are used because the time that is required for each forward simulation is short (a minute or less). Thus, many simulations, thousands in this case, can be accomplished in a reasonably short time period. The effect of using 1-D columnar models is that all flow is forced to be vertical; no lateral flow is considered in these models. From the surface to the repository, lateral flow is not expected to be significant because perched water has not been found here. Below the repository, in the Calico Hills nonwelded unit (CHn: see Table 6) and the Crater Flat undifferentiated unit (CFu), areas of perched water exist where lateral flow may be significant. Properties needed to produce perched water and varying degrees of lateral flow are addressed in *UZ Flow Model and Submodels* (BSC 2001 [158726]). Properties for the zeolitic portion of CHn, the unit where perched water is observed, are not calibrated here. Fracture permeability and van Genuchten *m* are not calibrated here because they are expected to be relatively insensitive to simulated matrix-saturation and water-potential distributions. A detailed discussion of sensitivities of rock properties to the relevant simulation results is provided by Bandurraga and Bodvarsson (1999 [103949], Section 5). Nevertheless, reduction in the number of calibrated properties is necessary because of the limited data points available for inversions. A total of 78 rock parameters are to be estimated. This set of parameters is chosen for calibration because it is a relatively small set that could represent ambient conditions in the UZ.

Residual and satiated saturation are parameters that do not influence the calibration to ambient data as strongly as the van Genuchten parameter α. This is because ambient saturation and water-potential data are generally not at the extremes of the relationships where these bounding values play a stronger role. Like matrix porosity, matrix residual saturation is another property that is simple to measure with low error, so it makes more sense to calibrate the parameters that are not well constrained.

The matrix van Genuchten *m* parameter, which is essentially a pore-size distribution index, is well constrained by the desaturation data (Table 3), whereas the same data may give an estimate of the van Genuchten α that is biased toward the drainage condition. In this study, matrix van Genuchten *m* parameters are not calibrated. This reduces the number of parameters in the calibration.

Other hydrological parameters not calibrated are fracture and matrix porosity, residual saturation, and satiated saturation. Liquid flow simulations, because they are in steady state, are insensitive to porosity variations, so porosity could not be calibrated by inversion of saturation and water-potential data. Further, matrix porosity is a well-constrained property because the techniques used to measure porosity are simple and the measurement error is low.

Because there are no data for model layers tr3 and tr2, they are assigned the same properties as model layers bf3 and bf2, respectively (Assumption 1, in Section 5). This assignment is based on the common depositional profile of the Tram and Bullfrog Tuffs. Because the Bullfrog Tuff represents a very small portion of the UZ within the UZ Model boundaries (it is present above

the water table only immediately next to the Solitario Canyon fault and in the extreme northern portion of the UZ Model) (BSC 2003 [160109], Section 6), the impact of this approximation is not significant.

Common values of k_M, α_M, α_F, are used for the vitric Tac (material types ch2v, ch3v, ch4v, and ch5v) and for the zeolitic Tac (material types ch2z, ch3z, ch4z, and ch5z), respectively. The common value refers to a property value shared by several model layers. As reflected in Table 6, these layers do not represent actual geologic or hydrogeologic divisions, but are employed to better characterize which portions of the Tac are vitric or zeolitic, as documented in the Scientific Analysis report *Development of Numerical Grids for UZ Flow and Transport Modeling* (BSC 2003 [160109], Section 6).

The lower nonlithophysal layer of the TSw (Tptpln) is subdivided into two layers based on matrix property development consistent with Flint (1998 [100033], pp. 27–29). This division does not exist for the fracture properties (see Table 4), so common values of fracture properties are used for material types tsw36 and tsw37.

The fracturing characteristics of the rocks of Yucca Mountain are considered to be primarily dependent on the degree of welding and alteration. Data in Table 4 show that this is true of fracture frequency. The welded rocks have higher fracture frequencies than nonwelded rocks. Because of the general division between the fracture characteristics of welded and nonwelded rocks, model layers are grouped together, based on welding, to estimate common values of the active fracture parameter. Alteration is believed to possibly influence the active fracture parameter, so it is also used as a criterion for grouping layers. Common values of γ are estimated for the TCw, PTn, some layers of the TSw, zeolitic portions of the TSw, CHn and CFu, and devitrified/welded portions of the CHn and CFu. Table 10 shows the material types included in each of these groups. The value of γ is estimated individually for tsw31 because matrix-to-fracture flow is expected to be high in this layer, as a result of the transition from matrix-dominated flow in the PTn to fracture-dominated flow in the TSw. No prior information exists for the active fracture parameter, γ. Initial estimates for γ are taken as 0.25 for all layers, as shown in Table 10.

Table 10. Initial Estimates of the Active Fracture Parameter, γ, for Saturation and Water-Potential Data Inversion

Material Type (group)	γ
tcw11, tcw12, tcw13	0.25
ptn21, ptn22, ptn23, ptn24, ptn25, ptn26	0.25
tsw31	0.25
tsw32 and tsw33	0.25
tsw34, tsw35, tsw36, tsw37, tsw38, tsw39	0.25
ch1z, ch2z, ch3z, ch4z, ch5z, ch6, pp4, pp1, bf2 and tswz (zeolitic portion of tsw39)	0.25
pp3, pp2, bf3	0.25

Output-DTNs: LB0208UZDSCPLI.001; LB0208UZDSCPMI.001

Prior information (Section 6.2.4) is used as initial guesses of inversions, except for the upper infiltration case. For that case, numerical convergence is difficult to obtain, and therefore the calibrated drift-scale property set for the base-case infiltration scenario is used as initial guesses. Fracture permeabilities for pp4 and pp3 are adjusted.

Calibration Results—The one-dimensional calibrated drift-scale parameter set for the base-case (mean) infiltration scenario is presented in Table 11. Matches to the saturation data achieved with this parameter set for USW SD-9 are shown in Figure 2. Note that a comparison between data and simulation results for the zeolitic portion of CHn is not shown because saturation data there are not used for calibration. Figure 3 shows matches to the water-potential data for USW SD-12. The objective function value for this run is 0.46E+4 (that is, 0.46×10^4).

The one-dimensional calibrated parameter set for the upper-bound infiltration scenario is presented in Table 12. Matches to the saturation data achieved with this parameter set for USW SD-9 are shown for saturation in Figure 4. Note that a comparison between data and simulation results for the zeolitic portion of CHn is not shown because saturation data from that location are not used for calibration. Figure 5 shows matches to the water-potential data for USW SD-12. The objective function value for this run is 0.59E+4.

The one-dimensional calibrated parameter set for the lower-bound infiltration scenario is presented in Table 13. Matches to the saturation data achieved with this parameter set for USW SD-9 are shown for saturation in Figure 6. Note that a comparison between data and simulation results for zeolitic portion of CHn is not shown because saturation data from that location are not used for calibration. Figure 7 shows matches to the water-potential data for USW SD-12. The objective function value for this run is 0.62E+4.

Table 11. Calibrated Parameters from One-Dimensional Inversion of Saturation, and Water-Potential Data for the Base-Case Infiltration Scenario*

Model Layer	K_M (m^2)	α_M (1/Pa)	m_M (-)	K_F (m^2)	α_F (1/Pa)	m_F (-)	γ (-)
tcw11	3.74E-15	1.01E-5	0.388	3.0E-11	5.27E-3	0.633	0.587
tcw12	5.52E-20	3.11E-6	0.280	5.3E-12	1.57E-3	0.633	0.587
tcw13	5.65E-17	3.26E-6	0.259	4.5E-12	1.24E-3	0.633	0.587
ptn21	4.60E-15	1.62E-4	0.245	3.2E-12	8.70E-4	0.633	0.232
ptn22	4.43E-12	1.46E-4	0.219	3.0E-13	1.57E-3	0.633	0.232
ptn23	9.20E-15	2.47E-5	0.247	3.0E-13	5.18E-3	0.633	0.232
ptn24	2.35E-12	7.90E-4	0.182	3.0E-12	1.86E-3	0.633	0.232
ptn25	2.15E-13	1.04E-4	0.300	1.7E-13	1.33E-3	0.633	0.232
ptn26	1.00E-11	9.83E-4	0.126	2.2E-13	1.34E-3	0.633	0.232
tsw31	2.95E-17	8.70E-5	0.218	8.1E-13	1.60E-5	0.633	0.129
tsw32	2.23E-16	1.14E-5	0.290	7.1E-13	1.00E-4	0.633	0.600
tsw33	6.57E-18	6.17E-6	0.283	7.8E-13	1.59E-3	0.633	0.600
tsw34	1.77E-19	8.45E-6	0.317	3.3E-13	1.04E-4	0.633	0.569
tsw35	4.48E-18	1.08E-5	0.216	9.1E-13	1.02E-4	0.633	0.569
tsw36	2.00E-19	8.32E-6	0.442	1.3E-12	7.44E-4	0.633	0.569
tsw37	2.00E-19	8.32E-6	0.442	1.3E-12	7.44E-4	0.633	0.569
tsw38	2.00E-18	6.23E-6	0.286	8.1E-13	2.12E-3	0.633	0.569
tswz (zeolitic portion of tsw39)	3.5E-17	4.61E-6	0.059	8.1E-13	1.5E-3	0.633	0.370 [d]
tswv (vitric portion of tsw39)	1.49E-13	4.86E-5	0.293	a	a	a	a
ch1z	3.5E-17	2.12E-7	0.349	2.5E-14	1.4E-3	0.633	0.370 [d]
ch1v	6.65E-13	8.73E-5	0.240	a	a	a	a
ch2v	2.97E-11	2.59E-4	0.158	a	a	a	a
ch3v	2.97E-11	2.59E-4	0.158	a	a	a	a
ch4v	2.97E-11	2.59E-4	0.158	a	a	a	a
ch5v	2.97E-11	2.59E-4	0.158	a	a	a	a
ch6v	2.35E-13	1.57E-5	0.147	a	a	a	a
ch2z	5.2E-18	2.25E-6	0.257	2.5E-14	8.9E-4	0.633	0.370 [d]
ch3z	5.2E-18	2.25E-6	0.257	2.5E-14	8.9E-4	0.633	0.370 [d]
ch4z	5.2E-18	2.25E-6	0.257	2.5E-14	8.9E-4	0.633	0.370 [d]
ch5z	5.2E-18	2.25E-6	0.257	2.5E-14	8.9E-4	0.633	0.370 [d]
ch6z	8.2E-19	1.56E-7	0.499	2.5E-14	1.4E-3	0.633	0.370 [d]
pp4	8.77E-17	4.49E-7	0.474	2.5E-14	1.83E-3	0.633	0.370
pp3	7.14E-14	8.83E-6	0.407	2.2E-13	2.47E-3	0.633	0.199
pp2	1.68E-15	2.39E-6	0.309	2.2E-13	3.17E-3	0.633	0.199
pp1	2.35E-15	9.19E-7	0.272	2.5E-14	1.83E-3	0.633	0.370 [d]
bf3	4.34E-13	1.26E-5	0.193	2.2E-13	2.93E-3	0.633	0.199
bf2	8.1E-17	1.18E-7	0.617	2.5E-14	8.9E-4	0.633	0.370 [d]

NOTE: * These data have been developed as documented in this Model Report and submitted under Output-DTN: LB0208UZDSCPMI.002. Not all the properties in this table are fixed (i.e., not allowed to change) in calibration (Section 6.3.2). Fixed property values are directly taken from Tables 3 and 4.

a = Calibrated Properties Model conceptual model does not include fractures in these model layers (Section 5).

[d] = The γ parameter was not calibrated for those layers. The value from pp4 is assigned to these layers.

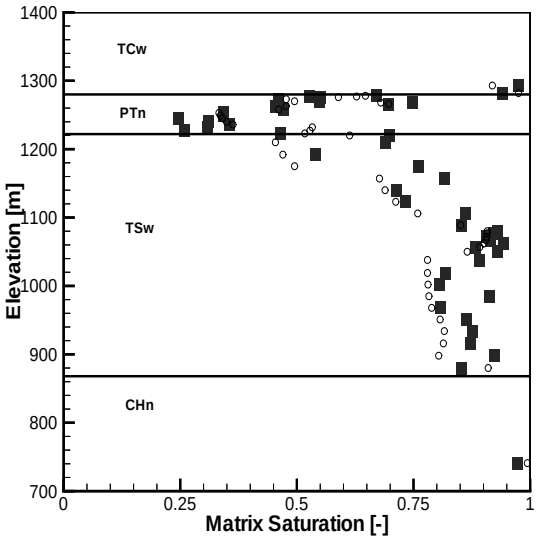

Output-DTN: LB0208UZDSCPMI.001

NOTE: Filled squares correspond to averaged core data and circles to simulation results.

Figure 2. Saturation Matches at USW SD-9 for One-Dimensional, Drift-Scale, Calibrated Parameter Set for the Base-Case Infiltration Scenario

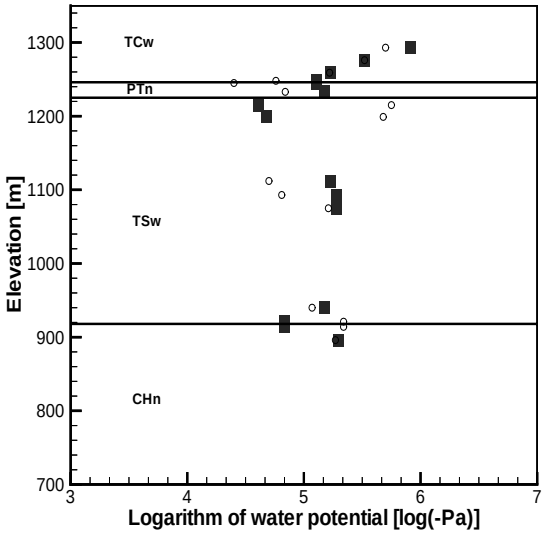

Output-DTN: LB0208UZDSCPMI.001

NOTE: Filled squares correspond to data and circles to simulation results.

Figure 3. Water-Potential Matches at USW SD-12 for One-Dimensional, Drift-Scale, Calibrated Parameter Set for the Base-Case Infiltration Scenario

Table 12. Calibrated Parameters from One-Dimensional Inversion of Saturation, and Water-Potential Data for the Upper-Bound Infiltration Scenario*

Model Layer	K_M (m^2)	α_M (1/Pa)	m_M (-)	K_F (m^2)	α_F (1/Pa)	m_F (-)	γ (-)
tcw11	3.90E-15	1.23E-5	0.388	3.0E-11	5.01E-3	0.633	0.500
tcw12	1.16E-19	3.39E-6	0.280	5.3E-12	2.19E-3	0.633	0.500
tcw13	4.41E-16	3.25E-6	0.259	4.5E-12	1.86E-3	0.633	0.500
ptn21	2.14E-14	1.56E-4	0.245	3.2E-12	2.69E-3	0.633	0.100
ptn22	1.29E-11	1.33E-4	0.219	3.0E-13	1.38E-3	0.633	0.100
ptn23	4.07E-14	2.39E-5	0.247	3.0E-13	1.23E-3	0.633	0.100
ptn24	4.27E-12	5.62E-4	0.182	3.0E-12	2.95E-3	0.633	0.100
ptn25	1.01E-12	9.48E-5	0.300	1.7E-13	1.10E-3	0.633	0.100
ptn26	1.00E-11	5.23E-4	0.126	2.2E-13	9.55E-4	0.633	0.100
tsw31	1.77E-17	4.85E-5	0.218	8.1E-13	1.58E-5	0.633	0.100
tsw32	2.13E-16	1.96E-5	0.290	7.1E-13	1.00E-4	0.633	0.561
tsw33	2.39E-17	5.22E-6	0.283	7.8E-13	1.58E-3	0.633	0.561
tsw34	2.96E-19	1.65E-6	0.317	3.3E-13	1.00E-4	0.633	0.570
tsw35	8.55E-18	5.03E-6	0.216	9.1E-13	5.78E-4	0.633	0.570
tsw36	7.41E-19	1.08E-6	0.442	1.3E-12	1.10E-3	0.633	0.570
tsw37	7.41E-19	1.08E-6	0.442	1.3E-12	1.10E-3	0.633	0.570
tsw38	7.40E-18	5.58E-6	0.286	8.1E-13	8.91E-4	0.633	0.570
tswz (zeolitic portion of tsw39)	3.5E-17	4.61E-6	0.059	8.1E-13	1.5E-3	0.633	0.500[d]
tswv (vitric portion of tsw39)	2.24E-13	4.86E-5	0.293	a	a	a	a
ch1z	3.5E-17	2.12E-7	0.349	2.5E-14	1.4E-3	0.633	0.500[d]
ch1v	1.39E-12	8.82E-5	0.240	a	a	a	a
ch2v	4.90E-11	2.73E-4	0.158	a	a	a	a
ch3v	4.90E-11	2.73E-4	0.158	a	a	a	a
ch4v	4.90E-11	2.73E-4	0.158	a	a	a	a
ch5v	4.90E-11	2.73E-4	0.158	a	a	a	a
ch6v	2.72E-13	1.67E-5	0.147	a	a	a	a
ch2z	5.2E-18	2.25E-6	0.257	2.5E-14	8.9E-4	0.633	0.500[d]
ch3z	5.2E-18	2.25E-6	0.257	2.5E-14	8.9E-4	0.633	0.500[d]
ch4z	5.2E-18	2.25E-6	0.257	2.5E-14	8.9E-4	0.633	0.500[d]
ch5z	5.2E-18	2.25E-6	0.257	2.5E-14	8.9E-4	0.633	0.500[d]
ch6z	8.2E-19	1.56E-7	0.499	2.5E-14	1.4E-3	0.633	0.500[d]
pp4	1.02E-15	4.57E-7	0.474	2.5E-12	8.91E-4	0.633	0.500
pp3	1.26E-13	9.50E-6	0.407	2.2E-12	1.66E-3	0.633	0.500
pp2	1.70E-15	2.25E-6	0.309	2.2E-13	1.66E-3	0.633	0.500
pp1	2.57E-15	8.77E-7	0.272	2.5E-14	8.91E-4	0.633	0.500[d]
bf3	3.55E-14	3.48E-5	0.193	2.2E-13	1.66E-3	0.633	0.500
bf2	8.1E-17	1.18E-7	0.617	2.5E-14	8.9E-4	0.633	0.500[d]

NOTE: * These data have been developed as documented in this Model Report and submitted under Output-DTN: LB0302UZDSCPUI.002. Not all the properties in this table are fixed (i.e., not allowed to change) in calibration (Section 6.3.2). Fixed property values are directly taken from Tables 3 and 4 (except fracture permeability for pp3 and pp4).

a = Calibrated Properties Model conceptual model does not include fractures in these model layers (Section 5).

[d] = The γ was not calibrated for these layers. The value from pp4 is assigned to these layers.

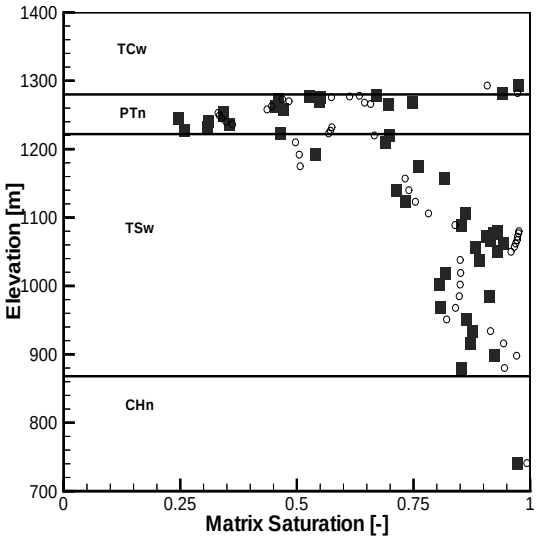

Output-DTN: LB0208UZDSCPUI.001

NOTE: Filled squares correspond to averaged core data and circles to simulation results.

Figure 4. Saturation Matches at USW SD-9 for One-Dimensional, Drift-Scale, Calibrated Parameter Set for the Upper-Bound Infiltration Scenario

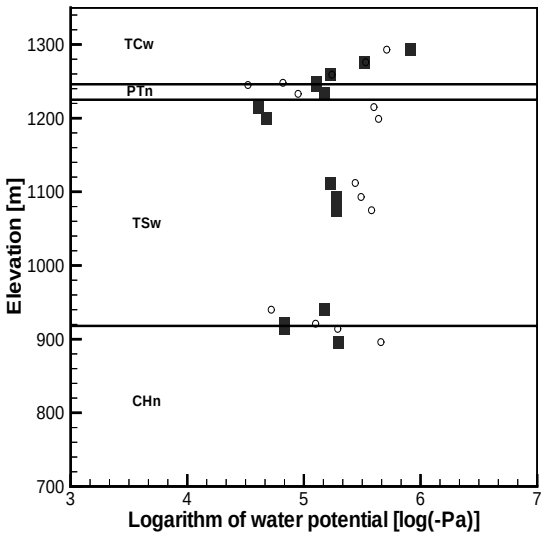

Output-DTN: LB0208UZDSCPUI.001

NOTE: Filled squares correspond to data and circles to simulation results.

Figure 5. Water-Potential Matches at USW SD-12 for a One-Dimensional, Drift-Scale, Calibrated Parameter Set for the Upper-Bound Infiltration Scenario

Table 13. Calibrated Parameters from One-Dimensional Inversion of Saturation and Water-Potential Data for the Lower-Bound Infiltration Scenario*

Model Layer	K_M (m^2)	α_M (1/Pa)	m_M (-)	K_F (m^2)	α_F (1/Pa)	m_F (-)	γ (-)
tcw11	3.44E-15	1.16E-5	0.388	3.0E-11	4.68E-3	0.633	0.483
tcw12	3.00E-20	2.67E-6	0.280	5.3E-12	3.20E-3	0.633	0.483
tcw13	3.96E-17	1.64E-6	0.259	4.5E-12	2.13E-3	0.633	0.483
ptn21	5.55E-15	6.38E-5	0.245	3.2E-12	2.93E-3	0.633	0.065
ptn22	8.40E-12	1.67E-4	0.219	3.0E-13	6.76E-4	0.633	0.065
ptn23	1.92E-14	4.51E-5	0.247	3.0E-13	3.96E-3	0.633	0.065
ptn24	6.66E-13	2.52E-3	0.182	3.0E-12	2.51E-3	0.633	0.065
ptn25	1.96E-14	1.24E-4	0.300	1.7E-13	1.53E-3	0.633	0.065
ptn26	1.00E-11	1.63E-3	0.126	2.2E-13	1.52E-3	0.633	0.065
tsw31	1.42E-17	8.02E-5	0.218	8.1E-13	1.58E-5	0.633	0.037
tsw32	3.96E-16	9.46E-6	0.290	7.1E-13	1.31E-4	0.633	0.528
tsw33	1.60E-18	4.25E-6	0.283	7.8E-13	1.94E-3	0.633	0.528
tsw34	1.38E-19	1.19E-6	0.317	3.3E-13	6.55E-4	0.633	0.476
tsw35	2.33E-18	1.97E-6	0.216	9.1E-13	1.35E-3	0.633	0.476
tsw36	5.58E-19	4.22E-7	0.442	1.3E-12	1.31E-3	0.633	0.476
tsw37	5.58E-19	4.22E-7	0.442	1.3E-12	1.31E-3	0.633	0.476
tsw38	2.93E-18	1.43E-6	0.286	8.1E-13	1.75E-3	0.633	0.476
tswz (zeolitic portion of tsw39)	3.5E-17	4.61E-6	0.059	8.1E-13	1.5E-3	0.633	0.276 [d]
tswv (vitric portion of tsw39)	3.15E-13	1.86E-5	0.293	a	a	a	a
ch1z	3.5E-17	2.12E-7	0.349	2.5E-14	1.4E-3	0.633	0.276 [d]
ch1v	3.15E-14	4.50E-5	0.240	a	a	a	a
ch2v	1.13E-11	1.22E-4	0.158	a	a	a	a
ch3v	1.13E-11	1.22E-4	0.158	a	a	a	a
ch4v	1.13E-11	1.22E-4	0.158	a	a	a	a
ch5v	1.13E-11	1.22E-4	0.158	a	a	a	a
ch6v	2.54E-13	9.05E-6	0.147	a	a	a	a
ch2z	5.2E-18	2.25E-6	0.257	2.5E-14	8.9E-4	0.633	0.276 [d]
ch3z	5.2E-18	2.25E-6	0.257	2.5E-14	8.9E-4	0.633	0.276 [d]
ch4z	5.2E-18	2.25E-6	0.257	2.5E-14	8.9E-4	0.633	0.276 [d]
ch5z	5.2E-18	2.25E-6	0.257	2.5E-14	8.9E-4	0.633	0.276 [d]
ch6z	8.2E-19	1.56E-7	0.499	2.5E-14	1.4E-3	0.633	0.276 [d]
pp4	2.98E-16	2.88E-7	0.474	2.5E-14	1.88E-3	0.633	0.276
pp3	5.37E-14	7.97E-6	0.407	2.2E-13	1.32E-3	0.633	0.248
pp2	4.24E-16	2.41E-6	0.309	2.2E-13	2.80E-3	0.633	0.248
pp1	7.02E-16	1.36E-6	0.272	2.5E-14	6.39E-4	0.633	0.276 [d]
bf3	2.97E-14	1.32E-5	0.193	2.2E-13	1.91E-3	0.633	0.248
bf2	8.1E-17	1.18E-7	0.617	2.5E-14	8.9E-4	0.633	0.276 [d]

NOTE: * These data have been developed as documented in this Model Report and submitted under Output-DTN: LB0208UZDSCPLI.002. Not all the properties in this table are varied in calibration (Section 6.3.2). Fixed property values are directly taken from Tables 3 and 4.

a = Calibrated Properties Model conceptual model does not include fractures in these model layers (Section 5).

[d] = The γ parameter was not calibrated for these layers. The value from pp4 is assigned to these layers.

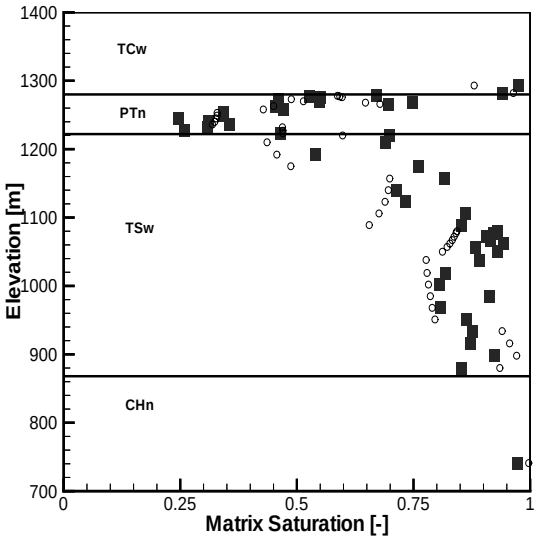

Output-DTN: LB0208UZDSCPLI.001

NOTE: Filled squares correspond to averaged core data and circles to simulation results.

Figure 6. Saturation Matches at USW SD-9 for a One-Dimensional, Drift-Scale, Calibrated Parameter Set for the Lower-Bound Infiltration Scenario

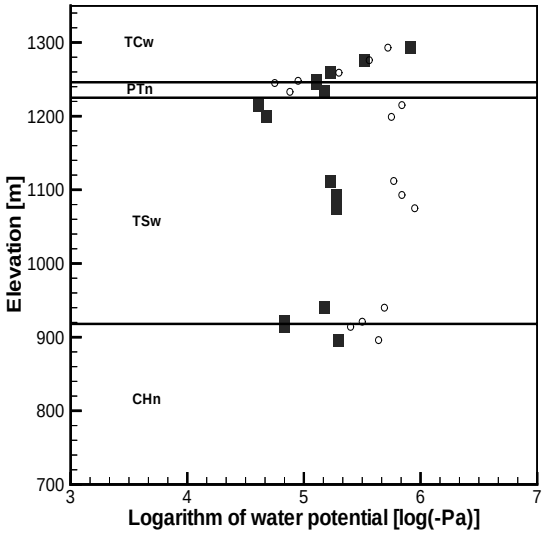

Output-DTN: LB0208UZDSCPLI.001

NOTE: Filled squares correspond to data and circles to simulation results.

Figure 7. Water-Potential Matches at USW SD-12 for a One-Dimensional, Drift-Scale, Calibrated Parameter Set for the Lower-Bound Infiltration Scenario

6.3.3 Calibration of Mountain-Scale Parameters

Scale Dependence of Fracture Permeability—It is well documented in the literature that large-scale effective permeabilities are generally larger than smaller-scale ones (Neuman 1994 [105731]). An intuitive explanation for this scale-dependent behavior is that a large observation scale, in an average sense, corresponds to a larger opportunity to encounter more permeable zones or paths when observations are made, which considerably increases values of the observed permeability. Because of the scale difference, drift-scale fracture permeabilities, determined from air-injection tests, cannot be applied to mountain-scale modeling. Therefore, development of mountain-scale properties is needed. In addition to matching matrix-saturation and water-potential data, the determination of mountain-scale parameters also involves matching pneumatic pressure data measured in surface boreholes. In the drift-scale parameter sets, fracture permeabilities correspond to those determined from air-injection tests. The pneumatic pressure data result from mountain-scale gas-flow processes, while air-injection tests correspond to scales on an order of several meters or less.

Unlike the connected fracture networks and soils, studies on the scale-dependent behavior of matrix properties in unsaturated fractured rocks are very limited. However, it is reasonable to believe that the scale-dependent behavior of the matrix is different from fracture networks. For example, relatively large fractures can act as capillary barriers for flow between matrix blocks separated by these fractures, even when the matrix is essentially saturated (water potential is close to the air entry value). This might limit the matrix scale-dependent behavior to a relatively small scale associated with the spacing between relatively large fractures. Although it is expected that estimated large-scale matrix permeabilities should be larger than those measured on a core-scale, no evidence exists to indicate that matrix properties should be very different on both the site and drift scales, which are much larger than the scale characterized by the fracture spacing. This point is also supported by the inversion results for the drift-scale properties. For example, the estimated drift-scale matrix permeabilities are generally much closer to prior information than estimated site-scale fracture permeabilities.

Based on the above discussions, only fracture permeabilities for the mountain-scale property sets are recalibrated, whereas other properties remain the same as those in the corresponding drift-scale properties. The calibration includes three steps: (1) fracture permeabilities are calibrated by matching the pneumatic pressure data; (2) the matches to matrix-saturation and water-potential data are checked using parameter sets that include calibrated fracture permeabilities; and (3) if the matches are not maintained, a new calibration using matrix-saturation and water-potential data would be needed for fracture permeabilities. These steps may need to be repeated until parameter sets match both pneumatic pressure data and matrix-saturation/water-potential data. As can be seen, this calibration is an iterative process.

Calibration Procedure Using Pneumatic Pressure Data—The EOS3 module of iTOUGH2 V5.0 (LBNL 2002 [160106]) is used for transient pneumatic simulations. Both the gas phase and the liquid phase are considered in the flow calculations. The pneumatic inversion is carried out in two steps. First, the fracture permeabilities for layers tcw11 through ptn26 are calibrated. Then, the permeabilities for layers tsw31 through 37 are calibrated as a group by multiplying the prior information for all seven layers by the same factor. The calibration activities are documented in the scientific notebook by Wang (2002 [160401], SN-LBNL-SCI-215-V1, pp. 71–80, 87–88).

The calibrated fracture permeabilities resulting from inversion of pneumatic data are expected to be higher than the prior information due to scale dependency of fracture permeabilities as described above. Therefore, the initial estimates for the fracture permeabilities are $10^{-10.5}$ m^2 for tcw11, tcw12, and tcw13, and $10^{-11.5}$ m^2 for ptn21 through ptn26. These estimates are higher than the corresponding prior information (Table 4). The permeabilities of layers tsw31 through 37 are set to the values previously calibrated using the pneumatic data (DTNs: LB997141233129.001 [104055], LB997141233129.002 [119933] and LB997141233129.003 [119940]).

The lack of significant attenuation in the TSw unit is considered an important feature shown by the gas pressure data. The calibrated fracture permeabilities for the model layers in the TSw unit need to be consistent with this feature. Therefore, fracture permeabilities in the TSw need to be determined in such a way that the simulated and observed gas pressure signals at the upper and lower sensor locations in the TSw have similar degrees of attenuation for borehole USW SD-12. Borehole USW SD-12 is chosen for this analysis because the distance between the two TSw sensors within this borehole is the largest among all the relevant boreholes. The degree of attenuation of the barometric signal through the TSw in USW SD-12, or the relative difference between the signals at the two sensor locations, was determined by using standard functions of Excel 97 SR-1 (see description of QAd.xls in Attachment I) to evaluate

$$F = \frac{1}{N}\left\{\sum_{i=1}^{N}\left[\left(P_u(t_i) - P_u(t_1)\right) - \left(P_b(t_i) - P_b(t_1)\right)\right]^2\right\}^{1/2} \qquad \text{(Eq. 10)}$$

where N is the total number of calibration time points, P is the gas pressure, and subscripts u and b refer to the sensors in the upper and lower (bottom) portions of the TSw within borehole USW SD-12. Obviously, if the gas signals from the two sensors are identical, F should be equal to zero. For the USW SD-12 gas-signal data (DTN: LB991091233129.001 [125868]), the F value is 2.01E-3 (kPa). In this study, fracture permeabilities need to be determined that will predict F values similar to the value calculated from the data, such that the simulated and observed gas-pressure signals have similar degrees of attenuation.

Since the gas-pressure data from the TSw are relatively limited compared TCw and PTn units and the insignificant attenuation and time lag between the upper-most and lower-most sensors are used for calibration, the fracture permeabilities for different model layers in this unit could not be independently estimated in a reliable manner. Note that the attenuation and time lag are determined by the overall hydraulic properties between the two sensors, rather than by properties in a single model layer. Therefore, the ratios of the permeabilities of layers tsw31 through tsw37 are held constant, and the prior information permeability values are multiplied by a single factor, d. For a given infiltration map, a number of values, log(d), between 1 and 2 with an interval of 0.1 are tested to determine the d resulting in an F value closest to the F value corresponding to the data. To calculate an F value for a d factor, modelers used the outputs from the TCw and PTn fracture permeability calibrations to run the forward simulation using iTOUGH2 V5.0 (LBNL 2002 [160106]) for generating gas pressures used in Equation 10. In a forward simulation, all the rock properties are the same as those determined from the corresponding TCw and PTn fracture permeability calibration, except the fracture permeabilities for model layers tsw31 to tsw37 are determined using the d factor and the prior information.

The determined log(*d*) values based on the above procedure (derived from Output-DTN: LB02091DSSCP3I.001) are shown in Table 14 for the three infiltration maps. The log(*d*) values range from 1.8–2.0, indicating that the fracture permeabilities for the relevant model layers are increased by about two orders of magnitude compared to the prior information. This results from the scale effects, as previously discussed.

Table 14. The Calculated Log(*d*) Factors for the Three Infiltration Maps

Base-case	Upper Bound	Lower Bound
2.0	1.9	1.8

Source: Wang 2002 [160401], SN-LBNL-SCI-215-V1, p. 75

Table 15 provided mountain-scale fracture permeabilities calibrated with pneumatic pressure data for three infiltration scenarios.

Table 15. Calibrated Mountain-Scale Fracture Permeabilities (m^2)

Model Layer[a]	Basecase	Upper Bound	Lower Bound
tcw11	4.24E-11	3.16E-12	3.16E-12
tcw12	9.53E-11	1.00E-10	9.73E-11
tcw13	1.32E-11	9.67E-13	9.47E-13
ptn21	2.11E-11	1.00E-11	1.00E-11
ptn22	9.41E-12	3.85E-13	1.00E-11
ptn23	5.35E-13	9.04E-14	1.16E-13
ptn24	1.00E-11	3.16E-13	1.00E-11
ptn25	1.24E-12	1.59E-14	4.37E-13
ptn26	3.17E-13	9.23E-14	8.29E-14
tsw31	8.13E-11	6.46E-11	5.13E-11
tsw32	7.08E-11	5.62E-11	4.47E-11
tsw33	7.76E-11	6.17E-11	4.90E-11
tsw34	3.31E-11	2.63E-11	2.09E-11
tsw35	9.12E-11	7.24E-11	5.75E-11
tsw36	1.35E-10	1.07E-10	8.51E-11
tsw37	1.35E-10	1.07E-10	8.51E-11

NOTE: These data have been developed as documented in this Model Report and submitted under Output-DTN: LB02091DSSCP3I.002.
[a] In the numerical grids used in inversions, the name of (fracture) model layer is the same as the corresponding model layer name in the table except that the 4th character is "F".

Saturation and Water Potential Check—Matches to the saturation and water-potential data were checked and found to be satisfactory, because for a given infiltration scenario, the

objective-function values are almost identical for both the mountain-scale property set and the corresponding drift-scale property set (Wang 2002 [160401], SN-LBNL-SCI-215-V1, pp. 75–76). Therefore, no further adjustment is needed. This also further confirms the previous assertion that under ambient conditions, simulated matrix water potential and saturation distributions are insensitive to fracture permeability values.

Figure 8 shows pneumatic pressure matches at USW SD-12 for a one-dimensional, mountain-scale, calibrated parameter set for the base-case infiltration scenario. Similar matches are obtained for other boreholes and for two other infiltration scenarios. In Figure 8, both simulated and observed pressure curves for a given geologic layer (Tptrn and Tpbt2) are shifted an identical distance along the vertical axis to better display the matches.

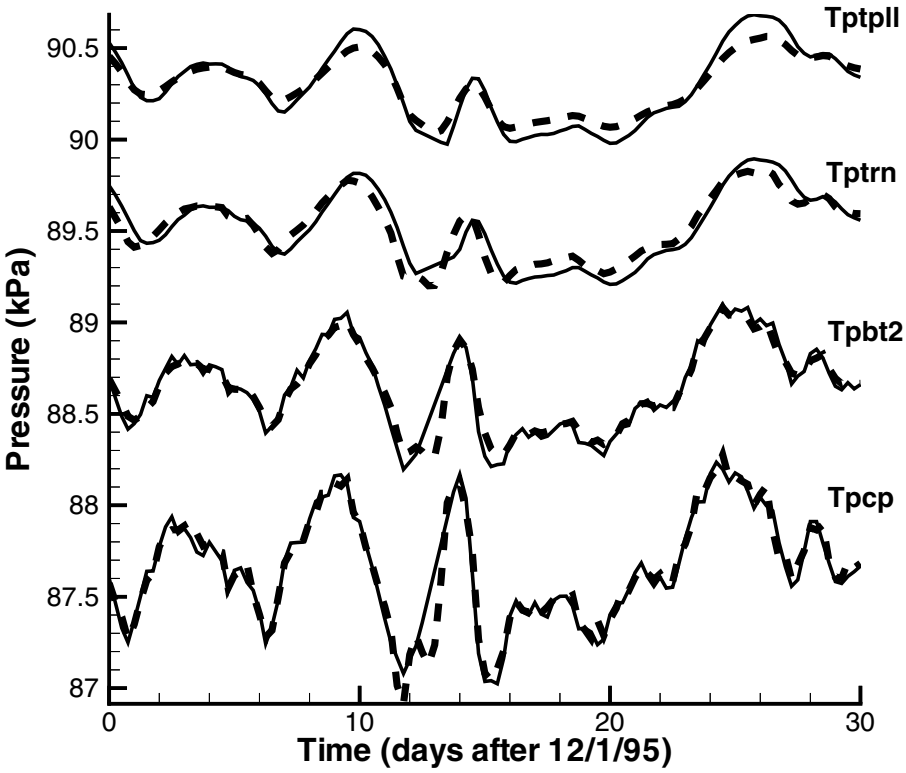

Output-DTN: LB02091DSSCP3I.001

NOTE: Solid lines correspond to the interpolated raw data and dashed lines to simulated results.

Figure 8. Pneumatic Pressure Matches at USW SD-12 for the One-Dimensional, Mountain-Scale, Calibrated Parameter Set for the Base-Case Infiltration Scenario

6.3.4 Calibration of Fault Parameters

Two-dimensional flow (vertical and east-west) is considered to adequately describe the flow patterns around borehole USW UZ-7a, used for fault property calibration. Inverse modeling is computationally intensive. For this reason, it is necessary to use the simplest model that will adequately simulate the system being modeled. For flow in and around a fault zone, a 2-D model is necessary to capture the interaction of the hanging wall, fault zone, and foot wall. An east-

west, vertical cross section through USW UZ-7a and the Ghost Dance fault captures this interaction. This cross section is aligned approximately parallel to the dip of the beds and parallel to the dip of the fault (perpendicular to the strike). Any lateral flow in or around the fault zone should follow the dip of the beds and the fault**.**

The data from borehole USW UZ-7a represent the most complete data set from within a fault zone. Saturation, water potential, and pneumatic data are available from the surface down into the TSw. Other data sets that are influenced by faults, from boreholes USW NRG-6, UE-25 UZ#4, and UE-25 UZ#5, include only pneumatic pressure data and are only relevant to the TSw. Because of the limited amount of data, it is best to characterize one fault as completely as possible and apply these properties to all other faults. This treatment is necessary because not enough data are available for other faults. The Ghost Dance fault, located near the east boundary of a repository block, is an important hydrogeological feature as a potential flow path for receiving lateral flows along eastwardly tilted layer interfaces.

Use of the Input Data—Data from USW UZ-7a are the most comprehensive with respect to faults. Saturation, water potential, and pneumatic pressure data are available within the Ghost Dance fault zone from the surface to the upper layers of the TSw. Pneumatic-only data (that show fault influence) are available from three other boreholes, but are not used in this analysis (rationale documented in Section 4.1.2.3). Because the data on faults are so limited, they are separated into four layers to reduce the number of parameters used to characterize the fault zones. The layers are the TCw, PTn, TSw, and CHn/CFu. Data for inversion are available for only the first three layers, so only the parameters of these layers are calibrated. Minimization of the objective function is the only criterion used for a successful calibration. The proportion of fracture flow to matrix flow specifically in the fault is not an element of the conceptual model.

Saturation, water potential, and pneumatic pressure data, which are inverted to obtain the calibrated parameter sets, are developed from files with extension prn, UZ7asat.xls, and UZ-7acap.xls from DTN: LB991091233129.003 [119902] so that they can be compared to the numerical grid in a way similar to that described in Section 6.2.2. However, because geologic layering data from USW UZ-7a are not included in the geologic model used to develop the numerical grid, there is no one-to-one correlation between the grid layer elevations and the geology of USW UZ-7a. This problem is overcome by interpolating the data onto the grid (see description of Excel file UZ-7asat1_02.xls in Attachment I).

The calculation for the average saturations from core and *in situ* water potentials and their weighting for the inversion is the same as described in Section 6.2.2, except for the necessity of interpolation (based on geology) to assign data to the appropriate model layers. Criteria identical to those used in selecting an appropriate time interval for the pneumatic data as described in Section 6.2.3 are used to select data from USW UZ-7a. Table 16 shows the dates, subunits, and elevations for the data that were used in the inversion. The procedure to calculate elevations is the same as that given in Section 6.2.3. Subunits are determined from the elevations of sensors and contacts between the subunits (file contacts00md.dat of DTN: MO0012MWDGFM02.002 [153777]). Subunits Tpc, Tpcpv1, Tpbt2, Tptrv3/2 and Tptrn correspond to sensors TCP1319, TCP 1325, TCP 1331, TCP 1337, and TCP 1343, respectively (DTN: GS960308312232.001 [105573]). As with the one-dimensional pneumatic inversion, data are taken from the lowest TCw instrument station, all instrument stations in the PTn, and in the TSw within the fault zone.

Three instrument stations in the footwall (below the fault zone) are not included in the inversion because they represent interactions at the edge of the fault on a subgridblock scale not captured by the UZ Model. The calibration activities are documented in scientific notebooks by Wang (2002 [160401], SN-LBNL-SCI-215-V1, pp. 81–86, 100; SN-LBNL-SCI-199-V1, pp. 98–99, 104).

Table 16. Pneumatic Pressure Data Used for Inversion

Borehole	Subunit	Dates	Elevation (m)
USW UZ-7a	Tpc	12/1 – 12/31/95	1243.0
	Tpcpv1	12/1 – 12/31/95	1232.3
	Tpbt2	12/1 – 12/31/95	1221.6
	Tptrv3/2	12/1 – 12/31/95	1213.4
	Tptrn	12/1 – 12/31/95	1177.8

DTN: GS960308312232.001 [105573]

Calibration Procedure—Data inversion for calibration of the fault parameters is carried out in the same sequence of steps used for the one-dimensional mountain-scale inversion. First, the saturation and water-potential data are inverted. Second, the pneumatic data are inverted. Third, the calibrated parameters are checked against the saturation and water-potential data and further calibrated if needed.

Note that fault properties to be calibrated are fracture properties, whereas matrix properties within fault zones are the same as those in nonfault zones (DTN: LB02081DKMGKID.001 [160108]). Fracture permeabilities are fixed during the saturation and water-potential inversion, and are the only parameters calibrated to the pneumatic data. Parameters to be calibrated against matrix-saturation and water-potential data are fracture α and active-fracture-model parameter γ.

The calibrated fracture α and active-fracture-model parameter γ for the base-case infiltration scenario are used as initial guesses for inversion of matrix-saturation and water-potential data for the other two infiltration scenarios. The resultant objective function values for the other two infiltration scenarios are almost the same as those obtained using the calibrated property set for the base-case infiltration scenario. With this in mind, investigators applied the calibrated fracture α and active-fracture-model parameter γ for the base-case infiltration scenario to the other two infiltration scenarios. Note that the same fracture m (0.633) as that for the nonfault zone (Table 4) is used here for the fault zone, because no specific fracture m data are available for the fault zone. As discussed in Section 6.3.2, fracture m is not expected to be sensitive to simulated matrix saturation and water potential distributions.

Using the parameter set from the matrix-saturation and water-potential calibration step, the fracture permeabilities are calibrated by inversion of the pneumatic data for the base-case infiltration scenario. Automated inversion successfully improves the objective function and provides a good match to the pneumatic data.

The fault parameters calibrated for the base-case infiltration scenario are checked to determine whether they are satisfactory for the other two infiltration scenarios. The objective function values for the two infiltration scenarios, determined with forward runs of iTOUGH2 V5.0

(LBNL 2002 [160106]), are even smaller than that for the base-case infiltration scenario. Therefore, a single calibrated fault parameter set is applied to all three infiltration scenarios. Finally, the calibrated fault parameters are used to check the matches with matrix-saturation and water-potential data for the three infiltration scenarios. For each infiltration scenario, the resultant objective function value is almost identical to that obtained from the matrix saturation and water-potential calibration step. Therefore, the matches are satisfactory.

Calibration Results—The calibrated fault parameter set is presented in Table 17. Matches to the data achieved with this parameter set for USW UZ-7a are shown for saturation in Figure 9, for water potential in Figure 10, and for pneumatic pressure in Figure 11. In Figure 11, both simulated and observed pressure curves for a given geologic layer (Tptrn, Tptrv3/2, Tpbt2 and Tpcpv1) are shifted along the vertical axis an identical distance to better display the matches. Note that the calibrated fracture permeabilities in the fault zone (Table 17) are generally higher than those for nonfault zones (Table 15), which is consistent with measurement results of LeCain et al. (2000 [144612], Summary).

Table 17. Calibrated Fault Parameters from Two-Dimensional Inversions of Saturation, Water Potential, and Pneumatic Data

Model Layer	k_F (m^2)	α_F (1/Pa)	m_F (-)	γ (-)
tcwf	9.77E-10	3.89E-3	0.633	0.40
ptnf	1.00E-10	2.80E-3	0.633	0.11
tswf	2.51E-11	3.16E-4	0.633	0.30
chnf	3.70E-13	2.30E-3	0.633	0.30

NOTE: Parameters for layer chnf are not calibrated. The prior information is taken from DTN: LB0207REVUZPRP.001 [159526].

These data have been developed as documented in this Model Report and submitted under Output-DTN: LB02092DSSCFPR.002.

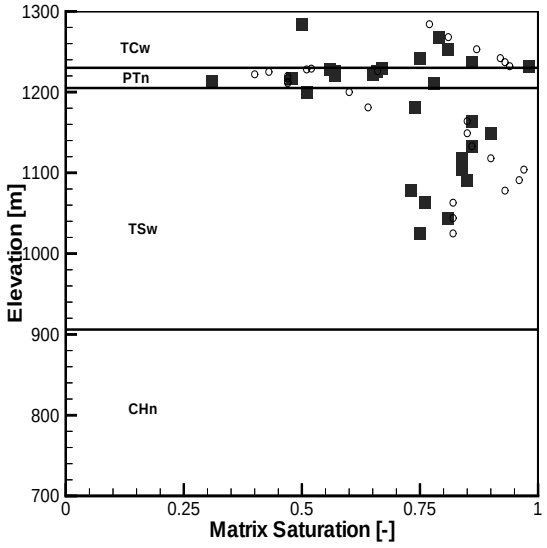

Output-DTN: LB02092DSSCFPR.001

NOTE: Filled squares correspond to averaged core data and circles to simulation results

Figure 9. Saturation Matches at USW UZ-7a used in the Two-Dimensional Calibrated Fault Parameter Set for the Base-Case Infiltration Scenario

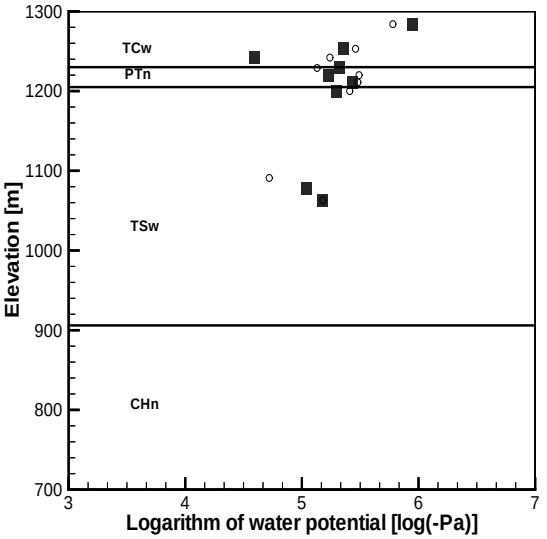

Output-DTN: LB02092DSSCFPR.001

NOTE: Filled squares correspond to data and circles to simulation results

Figure 10. Water-Potential Matches at USW UZ-7a used in the Two-Dimensional Calibrated Fault Parameter Set for the Base-Case Infiltration Scenario

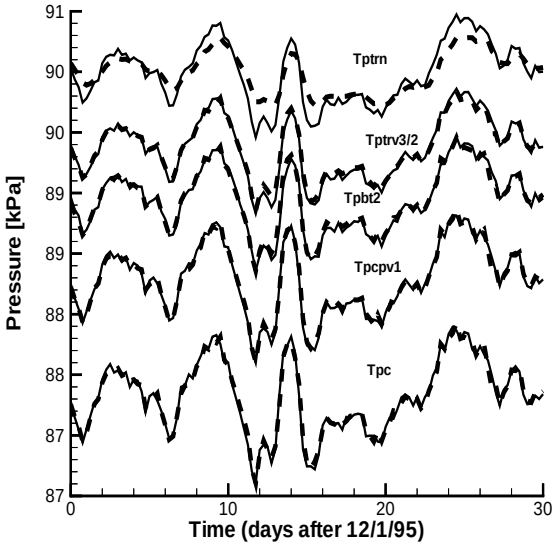

Output-DTN: LB02092DSSCFPR.001

NOTE: Solid lines correspond to the interpolated raw data and dashed lines to simulation results.

Figure 11. Pneumatic Pressure Matches at USW UZ-7a used in the Two-Dimensional Calibrated Fault Parameter Set for the Base-Case Infiltration Scenario

6.4 DISCUSSION OF PARAMETER UNCERTAINTY

This section discusses sources and quantification of uncertainties for the calibrated parameters.

6.4.1 Sources of Parameter Uncertainty

A major source of parameter uncertainty is the conceptual model. As previously discussed, the parameter calibration is based on the conceptual model for UZ flow and transport documented in *Conceptual and Numerical Models for UZ Flow and Transport* (CRWMS M&O 2000 [141187]). Some aspects of the conceptual model that are important for parameter calibration are presented in Section 6.1. Model simplifications used in this study will also contribute to parameter uncertainty. For example, 1-D models are used for calibrating drift-scale and mountain-scale property sets. As a result, lateral flow behavior in the UZ may not be captured by property sets determined from 1-D models.

Infiltration-rate uncertainty also contributes to parameter uncertainty, because flow processes in the UZ are largely determined by top boundary conditions. Using the three infiltration scenarios for the parameter calibration documented in this study captures this uncertainty.

In addition, scale effects are a well-known source of parameter uncertainty. This is especially true for determination of the UZ Model parameters. For example, matrix parameters are measured in the UZ at core scale on the order of several centimeters, whereas in the UZ Flow and Transport Model, numerical gridblocks are on the order of a few meters to hundreds of

meters. Scale-dependence of hydrologic parameters has been widely recognized in the scientific community (e.g., Neuman 1994 [105731]). This is also clearly indicated by the differences between calibrated and uncalibrated matrix properties, as shown in Table 18. Although upscaling is partially considered in developing uncalibrated matrix properties (DTN: LB0207REVUZPRP.002 [159672]), the calibrated matrix permeabilities are on average higher than uncalibrated ones for the three infiltration scenarios (Table 18). The general increase in permeability with scale is consistent with findings reported in the literature (e.g., Neuman 1994 [105731]). Consequently, the calibrated matrix α values are on average also higher than uncalibrated ones. A higher permeability is generally expected to correspond to a higher van Genuchten α. For example, fracture α values are significantly higher than matrix values. Scale-dependent behavior for fracture permeability is considered in this study by developing parameter sets at two different scales (mountain scale and drift scale). Calculation of the absolute residuals in Table 18 is documented in the scientific notebook by Wang (2002 [160401], SN-LBNL-SCI-215-V1, p. 90). The residuals for each layer (uncalibrated log x minus calibrated log x, where x = k_M or $\alpha_{M)}$ from Output-DTN: LB02091DSSCP3I.001 (files MGas_Ci.out, LGa_Ci.out and UGas_Ci.out) were averaged to calculate the values shown in Table 18. It should be emphasized that because of the difference between measurement scale and modeling scale, uncalibrated properties are not directly measured, but are in fact estimated values for the scales used in the UZ model. As a result, residuals cannot be used to evaluate the uncertainty as to the true parameter value, although they may be used to bound this uncertainty (as will be discussed below).

Table 18. Average Residual for Calibrated Matrix Properties for Three Infiltration Scenarios

	Residual for log(k_M)	**Residual for log(α_M)**
Base-case	-0.37	-0.25
Upper bound	-0.65	-0.17
Lower bound	-0.17	-0.06

Source: Wang 2002 [160401], SN-LBNL-SCI-215-V1, p. 90

NOTE: The residual refers to an uncalibrated matrix property minus the corresponding calibrated property.

Calibrated properties are non-unique because of data limitation. For example, in drift-scale parameter calibration, 78 parameters are calibrated to 300 data points. This is therefore a poorly constrained problem. Further complicating the calibrating process, many of the parameters are cross-correlated; that is, variations in two or more parameters may have the same effect on predicted system response. Because the problem is poorly constrained, there is no well-defined global minimum in the objective function. Rather, there are likely to be many equivalent local minima. With respect to moisture and water-potential data, any of these minima provide an equally good parameter set. To address this issue, this study uses uncalibrated parameters as initial guesses and prior information in most inversions.

Table 19. Average Absolute Residual for Calibrated Matrix Properties for Three Infiltration Scenarios

	Absolute Residual for log(k_M)	**Absolute Residual for log(α_M)**	**Absolute Residual for log(α_F)**
Base case	0.75	0.44	0.41
Upper bound	0.81	0.38	0.19
Lower bound	0.74	0.43	0.28

Source: Wang 2002 [160401], SN-LBNL-SCI-215-V1, p. 90

NOTE: The absolute residual refers to an absolute difference between uncalibrated matrix property and the corresponding calibrated property.

Table 19 shows the average absolute residual for calibrated matrix properties for three infiltration scenarios. The absolute value of the residual is always positive, and therefore the average absolute residual is greater than the average residual as shown in Table 18. The average standard deviation of log(k_M) for uncalibrated matrix property sets (prior information) (Table 3) is 1.61. The standard deviation for log(α_M) is not available from Table 3. Note that the standard errors for log(α_M) in Table 3 are determined from curve fitting (DTN: LB0207REVUZPRP.002 [159672]) and cannot be directly related to the corresponding standard deviations. Wang and Narasimhan (1993 [106793], pp. 374–376) reported that permeability could be approximately related to α by

$$k \propto \alpha^2 \qquad \text{(Eq. 11)}$$

This yields

$$\sigma_{\log(\alpha)} = \frac{1}{2}\sigma_{\log(k)} \qquad \text{(Eq. 12)}$$

where σ refers to standard deviation. Based on Equation 11, log(α) can be expressed as log(k)/2 plus a constant (for a given model layer), resulting in Equation 12. For each model layer, a standard deviation for log(α_M) can be estimated from the corresponding standard deviation of log(k_M) based on Equations 11 and 12. Average standard deviation (calculated by hand) for log(α_M) for the uncalibrated matrix property set (Table 3) is 0.81. The calculation of the residuals given in Table 19 and the standard deviations is documented in the scientific notebook by Wang (2002 [160401] SN-LBNL-SCI-215-V1, pp. 90–92). The absolute residual values (Table 19) for the matrix properties are smaller than the corresponding average standard deviations. The residual values for log(α_F) are also given in Table 19. They are close to or smaller than the average standard deviation of log(α_F) (0.30) determined from uncalibrated fracture property sets (Table 4) using Equation 12. All these support the appropriateness of the calibrated property sets documented in this report, which results from the use of uncalibrated rock properties as initial guesses and prior information in most inversions.

6.4.2 Quantification of Parameter Uncertainty

Quantifiable uncertainties are difficult to establish for the estimated parameter sets. In principle, these uncertainties could be evaluated either by Monte Carlo simulation or by linear error analysis, both of which are capabilities of iTOUGH2 V5.0 (LBNL 2002 [160106]). Because of the large numbers of parameters and the high nonlinearity of the unsaturated flow process, the linear error analysis is not reliable (Finsterle 1999 [104367]). The linear uncertainty analysis quantifies the parameter uncertainty by linearization (based on its first-order Taylor series expansion). This method is a powerful tool only for problems that have sufficiently small parameter uncertainties (e.g., a small number of parameters and a large number of data points for model calibration) or are linear (Finsterle 1999 [104367], Section 2.8.7). However, the problem under consideration is characterized by a large number of parameters (on the same order of data point number for drift-scale parameter calibrations) and high nonlinearity. The criteria for the linear uncertainty analysis to apply are not met for the problem under consideration. The sensitivity matrix evaluated at the solution and the resulting covariance matrix provide insight into the correlation structure of the estimated parameters, revealing strong interdependencies. This information is used to support the qualitative statements regarding estimation uncertainty. It also indicates that probabilistic statements about the confidence region around the best-estimate parameter set cannot be based on a linear uncertainty analysis, which assumes linearity and normality within that region (as previously discussed). Such statements would have no defensible basis. Evaluating the correct shape and extent of the confidence region would require mapping the objective function in the n-dimensional parameter space and determining the hypersurface corresponding to the appropriate confidence level. Such an approach is outlined (for two parameters only) in Finsterle and Pruess (1995 [161750]). Alternatively, Monte Carlo type methods (such as the bootstrap method) would be required. (The large number of parameters make uncertainty analysis by Monte Carlo simulation prohibitively time consuming.) Based on these considerations, the uncertainty information from prior information is believed to be more reliable (and practical) for determining uncertainties for the calibrated property sets.

In this study, parameter uncertainties (standard deviations) for the uncalibrated parameter sets (Tables 3 and 4) are directly used for the calibrated parameter sets, because these uncertainties are determined from measurements. The parameter uncertainty of the uncalibrated property sets are largely a result of small-scale spatial variability. Because the degree of spatial variability decreases with scale (subgrid scale [or high frequency] spatial variability is removed at a large scale), this is likely to provide upper limits of uncertainty on calibrated parameters for the given conceptual model and infiltration rates.

Table 20 gives the parameter uncertainties for the calibrated parameters. They are applied to both drift-scale and mountain-scale property sets because both scales are larger than those on which uncalibrated parameters were measured. Uncertainties for $\log(k_M)$, and $\log(k_F)$ are taken directly from Tables 3 and 4. When a $\log(k_F)$ uncertainty is not available in Table 4 for a model layer, the largest value among the uncertainties (standard deviations) in all the layers for which uncertainty values are available is used. Uncertainties for $\log(\alpha_M)$ and $\log(\alpha_F)$ are approximated from uncertainty values of the corresponding permeability, based on Equation 12. Uncertainties of the active-fracture-model parameter γ are difficult to obtain here and have not been calculated because prior information for γ is not available. Further discussions of the uncertainties of γ will be provided in other model reports describing analyses of hydrological properties data and UZ

flow model and submodels (BSC 2002 [160819], Sections 1.10.4 and I-1-1). No information is available for quantifying uncertainties for m_F that are not calibrated parameters (Section 6.3.2).

Table 20 also shows estimated uncertainties for calibrated fault properties taken from Table 4. Because fault properties are calibrated with limited data points (Section 6.3.4), the parameter uncertainties are expected to be relatively large. For each parameter type, the largest parameter uncertainty within the corresponding HGU for the nonfault property set is used as the corresponding fault parameter uncertainty. Note that the fault property set does not include matrix parameters.

Finally, it should be indicated that the propagation of uncertainty in model calibration is addressed in this study. The uncertainty data for measurements are used as inputs into inversions (Equation 1). The uncertainty in boundary conditions is reflected by developing property sets for different infiltration scenarios. The uncertainty in prior information has been used for characterizing uncertainties for calibrated properties.

Table 20. Uncertainties of Calibrated Parameters*

Model layer	Matrix Property		Fracture Property	
	Log(k_M)	Log(α_M)	Log(k_F)	Log(α_F)
tcw11	0.47	0.24	1.15	0.58
tcw12	2.74	1.37	0.78	0.39
tcw13	2.38	1.19	1.15	0.58
ptn21	2.05	1.03	0.88	0.44
ptn22	1.41	0.71	0.20	0.10
ptn23	0.64	0.32	0.20	0.10
ptn24	1.09	0.55	1.15	0.58
ptn25	0.39	0.20	0.10	0.05
ptn26	1.12	0.56	1.15	0.58
tsw31	3.02	1.51	1.15	0.58
tsw32	0.94	0.47	0.66	0.33
tsw33	1.61	0.81	0.61	0.31
tsw34	0.97	0.49	0.47	0.24
tsw35	1.65	0.83	0.75	0.38
tsw36	3.67	1.84	0.54	0.27
tsw37	3.67	1.84	0.28	0.14
tsw38	1.57	0.79	1.15	0.58
tswz (zeolitic portion of tsw39)	2.74	1.37	1.15	0.58
tswv (vitric portion of tsw39)	1.38	0.69	a	a
ch1z	2.74	1.37	1.15	0.58
ch1v	1.11	0.56	a	a
ch2v	1.62	0.81	a	a
ch3v	1.62	0.81	a	a
ch4v	1.62	0.81	a	a
ch5v	1.62	0.81	a	a
ch6v	1.11	0.56	a	a
ch2z	0.91	0.46	1.15	0.58
ch3z	0.91	0.46	1.15	0.58
ch4z	0.91	0.46	1.15	0.58
ch5z	0.91	0.46	1.15	0.58
ch6z	2.05	1.03	1.15	0.58
pp4	2.74	1.37	1.15	0.58
pp3	0.75	0.38	1.15	0.58
pp2	1.18	0.59	1.15	0.58
pp1	1.52	0.76	1.15	0.58
bf3	1.64	0.82	1.15	0.58
bf2	1.52	0.76	1.15	0.58
tcwf	b	b	1.15	0.58
ptnf	b	b	1.15	0.58
tswf	b	b	1.15	0.58
chnf	b	b	1.15	0.58

Output-DTN: LB0210AMRU0035.002
Input DTNs: LB0207REVUZPRP.002 [159672]; LB0205REVUZPRP.001 [159525]

NOTE: * These uncertainty values are taken or developed from Tables 3 and 4.
[a] = Calibrated Properties Model conceptual model does not include fractures in these model layers (Section 5)
[b] = Fault property set does not include matrix properties.

7. VALIDATION

7.1 THE VALIDATION CRITERIA

Validation activities for the Calibrated Properties Model are carried out based on *Technical Work Plan for: Performance Assessment Unsaturated Zone* (BSC 2002 [160819], Attachment I, Section I-1-1-1). A combination of several approaches are used for validation. First, the calibrated property sets are developed using a calibration methodology within experimental data sets (Section 6). Saturation data, *in situ* water potential data, pneumatic pressure data, and prior property information are inverted for the calibrations (Section 6). Matches to the data can be viewed as "cross-validation" of the Calibrated Properties Model. Second, the calibrated parameters are reviewed for reasonablessness. Calibrated parameters are consistent with the prior information, and the differences between them can be largely explained by the scale-dependency of rock properties (Section 6.4). Third, previous model calibration efforts using essentially the same methodology as used here have undergone technical review through publication in the open literature (Bandurraga and Bodvarsson 1999 [103949]; Bodvarsson et al. 2001 [160133]). Fourth, predictions using the Calibrated Properties Model are compared to data not used in the calibration process.

The focus of Section 7 is on the fourth validation activity. In this fourth activity, the Calibrated Properties Model predictions are compared to observed saturation, water potential, and pneumatic pressure data outside of calibration periods. The model will be accepted as valid for its purpose if all three of the following criteria are met (BSC 2002 [160819]. Attachment I, Section I-1-1-1): (1) for saturation data, the root-mean-square prediction errors (i.e., the difference between the validation data and the data predicted by the calibrated models) shall not exceed the greater of: 0.1 or three times the root-mean-square calibration errors (i.e., the difference between the data used in calibration and the simulation results from Calibrated Properties Model); (2) for water-potential data, the root-mean-square prediction errors (i.e., the differences between the validation data and the data predicted by the calibrated models) shall not exceed the greater of one order of magnitude of the water-potential data or three times the root-mean-square calibration errors (i.e., the difference between the validation data and the data predicted by the calibrated models); (3) for pneumatic pressure data, the root mean square prediction errors (i.e., the differences between the validation data and the data predicted by the calibrated models) shall not exceed the greater of 10% of the magnitude of the measured pneumatic pressure or three times the root-mean-square calibration errors. Note that allowed prediction errors are larger than calibration errors, considering that prediction errors are obtained using data that are used for calibration.

7.2 THE CALIBRATED HYDROLOGICAL PROPERTIES AND THE VALIDATION APPROACHES

The calibrated hydrological properties are obtained by matching the observed data (saturation, *in situ* capillary pressure, and dynamic pneumatic pressure data) using the iTOUGH2 V5.0 (LBNL 2002 [160106]), which minimizes the objective function (a measure of the misfit between the iTOUGH2 V5.0 (LBNL 2002 [160106]) model output and the observed data) by automatically adjusting hydrological property values. For validation purposes, we use

root-mean-square error (RMSE) between the model output and the data to describe the misfit between the iTOUGH2 V5.0 (LBNL 2002 [160106]) model (the numerical model of UZ) and the real system (the UZ at Yucca Mountain). The corresponding RMSE is called the *calibration residual* if the observed data were used in inversion (calibration activities). The calibration residual mainly reflects the errors in the conceptual model and the numerical schemes with respect to the real system. Measurement errors can also contribute to the calibration error. In all validation activities, mountain-scale calibrated property sets are used. For each infiltration scenario, a mountain-scale property set and the corresponding drift-scale property set give essentially the same matrix-saturation and water-potential distributions (Section 6.3.3). The observed raw pneumatic pressure data from the TDMS were taken at irregular time intervals. Therefore, iTOUGH2 V5.0 (LBNL 2002 [160106]) automatically interpolates the data to obtain a data set suitable for comparisons with simulation results. The averaged core saturation data at the gridblock scale (Section 6.2.2) are used in a simulation. These interpolated and averaged data are used in this section for calculating RMSE.

The validation approach used in this study involves predicting the Calibrated Properties Model's responses to present-day environments and comparing these responses to the available observed data not used in inversion (calibration activities). The prediction error (i.e., the corresponding RMSE between the model output and the observed data) is calculated to describe the accuracy of the calibrated model. The validation is performed using three data sets: saturation data, *in situ* capillary pressure data, and the dynamic pneumatic pressure data. The validation activities are also documented in scientific notebooks (Wang 2002 [160401], SN-LBNL-SCI-299-V1, pp. 9–21; SN-LBNL-SCI-215-V1, pp. 93–98). The Excel files, verification.xls and VGas.xls, are described in Attachment I. Data for model calibration and validation are selected in such a manner that adequate qualified data (especially data from deep boreholes) are used for calibration to obtain reliable calibrated property sets, and data that are not used for calibration and still contain important information about the UZ under ambient conditions are employed for validation to gain confidence of the Calibrated Properties Model.

Major aspects of the calibration methodology used in this study have been published in the open literature (Bandurraga and Bodvarsson 1999 [103949]; Bodvarsson et al. 2001 [160133]).

7.3 VALIDATION WITH OBSERVED SATURATION DATA

Table 9 lists boreholes from which matrix saturation data are used for calibration. The saturation data observed in the following boreholes are used in validation: USW SD-12, USW UZ-N32, USW UZ-N38, USW UZ-N54, USW UZ-N55, USW UZ-N58, and USW UZ-N59. The calculation of values for RMSE is presented in Verification.xls in Output DTN: LB0302AMRU0035.001 (See Attachment I).

Validation results are summarized in Table 21. In all three infiltration scenarios, the prediction errors are smaller than the corresponding calibration residuals. On average, the prediction error is 84% of the calibration residuals and much smaller than the validation criteria. Thus the Calibrated Properties Model can be accepted as valid in terms of predicting saturation.

Table 21. Validation in Terms of Saturation for Three Infiltration Scenarios

Infiltration scenario	Lower bound	Base case	Upper bound
Calibration residual (RMSE) [a]	0.1514	0.1343	0.1456
Prediction error (RMSE) [a]	0.1314	0.1094	0.1208
Validation Criteria [b]	<0.4542	<0.4029	<0.4368
Meet Criteria	Yes	Yes	Yes

Output-DTN: LB0210AMRU0035.002

NOTE: [a] RMSE—root mean square error (-)
[b] Validation Criteria—three times the calibration error

7.4 VALIDATION WITH OBSERVED *IN SITU* CAPILLARY PRESSURE DATA

The *in situ* capillary pressure data observed in the following boreholes were used in calibration: USW NRG-6, UE25 UZ#4, and USW SD-12 (Table 9). The *in situ* capillary pressure data observed in USW NRG-7a are used in validation. The calculation of values for RMSE is presented in Verification.xls in Output-DTN: LB0302AMRU0035.001 (see Attachment I).

These validation results are summarized in Table 22. In all three infiltration scenarios, the prediction errors are slightly larger than the corresponding calibration residual, but much smaller than the validation criteria, which are three times the calibration error. On average, the prediction error is 111% of the calibration residual. The validation criteria are met, and thus the Calibrated Properties Model can be accepted as valid in terms of predicting capillary pressure.

Table 22. Validation in Terms of Capillary Pressure for Three Infiltration Scenarios

Infiltration scenario	Lower bound	Base case	Upper bound
Calibration residual (RMSE) [a]	0.7181	0.4865	0.4402
Prediction error (RMSE) [a]	0.7250	0.4984	0.5736
Validation Criteria [b]	<2.1543	<1.4595	<1.3206
Meet Criteria	Yes	Yes	Yes

Output-DTN: LB0210AMRU0035.002

NOTE: [a] RMSE—root mean square error (log(Pa))
[b] Validation Criteria—three times the calibration error

7.5 VALIDATION WITH THE DYNAMIC PNEUMATIC PRESSURE DATA

The observed dynamic pneumatic pressure data in boreholes were collected from several time periods. Their usage for calibration and validation is summarized in Table 23. The calculation of values for RMSE is presented in VGas.xls in Output-DTN: LB0302AMRU0035.001 (see Attachment I).

Table 23. Usage of the Observed Dynamic Pneumatic Pressure Data

Borehole	DTN	Calibration period		Prediction period	
		Start	End	Start	End
USW NRG-7a	GS950208312232.003 [105572] GS951108312232.008 [106756] LB991091233129.001 [125868]	03/27/95	04/26/95	04/26/95	05/26/95
USW SD-12	GS960308312232.001 [105573] LB991091233129.001 [125868]	12/01/95	12/31/95	12/31/95	01/30/96
USW SD-7	GS960908312264.004 [106784] LB991091233129.001 [125868]	04/05/96	05/05/96	05/05/96	06/04/96
USW NRG-6	GS950208312232.003 [105572] GS951108312232.008 [106756] LB991091233129.001 [125868]	Not used	Not used	03/27/95	04/26/95

NOTE: (1) Only 25 days of data available for the sensor at Tpcpln of USW NRG-6, starting at 04/01/95.

(2) USW NRG-5 has been excluded in validation because data are not available beyond the calibration period.

Validation results are summarized in Table 24. The files surfbc3d.prn from DTN: LB02103DPNEUSM.001 [160250] is used as top boundary for gas pressure in the validation simulations. In all three infiltration scenarios, the prediction errors are slightly larger than the corresponding calibration residuals, but much smaller than the validation criteria, which are three times the calibration residual. On average, the prediction error is 149% of the calibration residual. The validation criteria are met. Thus, the Calibrated Properties Model can be accepted as valid in terms of predicting dynamic pneumatic pressure.

Table 24. Validation in Terms of Pneumatic Data for Three Infiltration Scenarios

Infiltration scenario	Lower bound	Base case	Upper bound
Calibration residual (RMSE)[a]	0.0832	0.0783	0.0870
Prediction error (RMSE)[a]	0.1131	0.1428	0.1124
Validation Criteria[b]	<0.2496	<0.2349	<0.2610
Meet Criteria	Yes	Yes	Yes

Output-DTN: LB0210AMRU0035.002

NOTE: [a] RMSE—root mean square error (kPa)
[b] Validation Criteria—three times the calibration error

In summary, the Calibrated Properties Model can be accepted as valid in terms of model predictions using different kinds of data. No further model validation activities are planned.

8. SUMMARY AND CONCLUSIONS

This report has documented the methodologies and the data used for developing rock property sets for three infiltration maps. Model calibration is necessary to obtain parameter values appropriate for the scale of the process being modeled. Although some hydrogeologic property data (prior information) are available, these data cannot be directly used to predict flow and transport processes because they were measured on scales smaller than those characterizing property distributions in models used for the prediction. Since model calibrations were done directly on the scales of interest, the upscaling issue was automatically considered. On the other hand, joint use of data and the prior information in inversions can further increase the reliability of the developed parameters compared with those for the prior information.

Rock parameter sets were developed for both the mountain and drift scales because of the scale-dependent behavior of fracture permeability. Note that these parameter sets, except those for faults, were determined using the 1-D simulations. Therefore, they cannot be directly used for modeling lateral flow because of perched water in the UZ of Yucca Mountain. Further calibration may be needed for two- and three-dimensional modeling studies.

As discussed above in Section 6.4, uncertainties for these calibrated properties are difficult to accurately determine, because of the inaccuracy of simplified methods for this complex problem or the extremely large computational expense of more rigorous methods. One estimate of uncertainty that may be useful to investigators using these properties is the uncertainty used for the prior information. In most cases, the inversions did not change the properties very much with respect to the prior information.

The Output DTNs (including the input and output files for all runs) from this study are given in Section 9.4.

INTENTIONALLY LEFT BLANK

9. INPUTS AND REFERENCES

The following is a list of the references cited in this document. Column 1 represents the unique six digit numerical identifier (the Document Input Reference System [DIRS] number), which is placed in the text following the reference callout (e.g., BSC 2002 [160819]). The purpose of these numbers is to assist the reader in locating a specific reference. Within the reference list, multiple sources by the same author (e.g., BSC 2002) are sorted alphabetically by title.

9.1 CITED DOCUMENTS

124842 Ahlers, C.F.; Finsterle, S.; and Bodvarsson, G.S. 1998. "Characterization and Prediction of Subsurface Pneumatic Pressure Variations at Yucca Mountain, Nevada." *Proceedings of the TOUGH Workshop '98, Berkeley, California, May 4-6, 1998*. Pruess, K., ed. LBNL-41995. Pages 222-227. Berkeley, California: Lawrence Berkeley National Laboratory. TIC: 247159.

103949 Bandurraga, T.M. and Bodvarsson, G.S. 1999. "Calibrating Hydrogeologic Parameters for the 3-D Site-Scale Unsaturated Zone Model of Yucca Mountain, Nevada." *Journal of Contaminant Hydrology, 38*, (1-3), 25-46. New York, New York: Elsevier. TIC: 244160.

103524 Bird, R.B.; Stewart, W.E.; and Lightfoot, E.N. 1960. *Transport Phenomena*. New York, New York: John Wiley & Sons. TIC: 208957.

160133 Bodvarsson, G.S.; Liu, H.H.; Ahlers, C.F.; Wu, Y-S.; and Sonnenthal, S. 2001. "Parameterization and Upscaling in Modeling Flow and Transport in the Unsaturated Zone of Yucca Mountain." Chapter 11 of *Conceptual Models of Flow and Transport in the Fractured Vadose Zone*. Washington, D.C.: National Academy Press. TIC: 252777.

159725 BSC (Bechtel SAIC Company) 2001. *Analysis of Hydrologic Properties Data*. ANL-NBS-HS-000002 REV 00 ICN 01. Las Vegas, Nevada: Bechtel SAIC Company. ACC: MOL.20020429.0296.

161316 BSC (Bechtel SAIC Company) 2001. *Calibrated Properties Model*. MDL-NBS-HS-000003 REV 00 ICN 01. Las Vegas, Nevada: Bechtel SAIC Company. ACC: MOL.20020311.0012.

158463 BSC (Bechtel SAIC Company) 2001. *In Situ Field Testing of Processes*. ANL-NBS-HS-000005 REV 01. Las Vegas, Nevada: Bechtel SAIC Company. ACC: MOL.20020108.0351.

160828 BSC (Bechtel SAIC Company) 2001. *Unsaturated Zone and Saturated Zone Transport Properties (U0100)*. ANL-NBS-HS-000019 REV 00 ICN 02. Las Vegas, Nevada: Bechtel SAIC Company. ACC: MOL.20020311.0017.

158726 BSC (Bechtel SAIC Company) 2001. *UZ Flow Models and Submodels*. MDL-NBS-HS-000006 REV 00 ICN 01. Las Vegas, Nevada: Bechtel SAIC Company. ACC: MOL.20020417.0382.

159124 BSC (Bechtel SAIC Company) 2002. *Geologic Framework Model (GFM2000)*. MDL-NBS-GS-000002 REV 01. Las Vegas, Nevada: Bechtel SAIC Company. ACC: MOL.20020530.0078.

160819 BSC (Bechtel SAIC Company) 2002. *Technical Work Plan for: Performance Assessment Unsaturated Zone*. TWP-NBS-HS-000003 REV 02. Las Vegas, Nevada: Bechtel SAIC Company. ACC: MOL.20030102.0108.

160319 BSC (Bechtel SAIC Company) 2002. *Thermal Conductivity of The Potential Repository Horizon Model Report.* MDL-NBS-GS-000005 REV 00. Las Vegas, Nevada: Bechtel SAIC Company. ACC: MOL.20020923.0167.

160109 BSC (Bechtel SAIC Company) 2003. *Development of Numerical Grids for UZ Flow and Transport Modeling*. ANL-NBS-HS-000015 REV 01. Las Vegas, Nevada: Bechtel SAIC Company. URN-1080

141187 CRWMS M&O (Civilian Radioactive Waste Management System Management and Operating Contractor) 2000. *Conceptual and Numerical Models for UZ Flow and Transport*. MDL-NBS-HS-000005 REV 00. Las Vegas, Nevada: CRWMS M&O. ACC: MOL.19990721.0526.

157916 Curry, P.M. and Loros, E.F. 2002. *Project Requirements Document*. TER-MGR-MD-000001 REV 00. Las Vegas, Nevada: Bechtel SAIC Company. ACC: MOL.20020806.0027.

159475 DOE (U.S. Department of Energy) 2002. *Quality Assurance Requirements and Description*. DOE/RW-0333P, Rev. 12. Washington, D.C.: U.S. Department of Energy, Office of Civilian Radioactive Waste Management. ACC: MOL.20020819.0387.

103783 Finsterle, S. 1998. *ITOUGH2 V3.2 Verification and Validation Report*. LBNL-42002. Berkeley, California: Lawrence Berkeley National Laboratory. ACC: MOL.19981008.0014.

104367 Finsterle, S. 1999. *ITOUGH2 User's Guide*. LBNL-40040. Berkeley, California: Lawrence Berkeley National Laboratory. TIC: 243018.

161750 Finsterle, S. and Pruess, K. 1995. "Solving the Estimation-Identification Problem in Two-Phase Flow Modeling." *Water Resources Research, 31*, (4), 913-924. Washington, D.C.: American Geophysical Union. TIC: 252318.

100033 Flint, L.E. 1998. *Characterization of Hydrogeologic Units Using Matrix Properties, Yucca Mountain, Nevada*. Water-Resources Investigations Report 97-4243. Denver, Colorado: U.S. Geological Survey. ACC: MOL.19980429.0512.

161743 Forsyth, P.A.; Wu, Y-S.; and Pruess, K. 1995. "Robust Numerical Methods for Saturated-Unsaturated Flow with Dry Initial Conditions in Heterogeneous Media." *Advances in Water Resources, 18*, 25-38. Southhampton, England: Elsevier. TIC: 235658.

139237 Glass, R.J.; Nicholl, M.J.; and Tidwell, V.C. 1996. *Challenging and Improving Conceptual Models for Isothermal Flow in Unsaturated, Fractured Rock Through Exploration of Small-Scale Processes*. SAND95-1824. Albuquerque, New Mexico: Sandia National Laboratories. ACC: MOL.19970520.0082.

144612 LeCain, G.D.; Anna, L.O.; and Fahy, M.F. 2000. *Results from Geothermal Logging, Air and Core-Water Chemistry Sampling, Air-Injection Testing, and Tracer Testing in the Northern Ghost Dance Fault, Yucca Mountain, Nevada, November 1996 to August 1998*. Water-Resources Investigations Report 99-4210. Denver, Colorado: U.S. Geological Survey. TIC: 247708.

160110 Liu, H.H. and Bodvarsson, G.S. 2001. "Constitutive Relations for Unsaturated Flow in a Fracture Network." *Journal of Hydrology, 252*, ([1-4]), 116-125. [New York, New York]: Elsevier. TIC: 253269.

105729 Liu, H.H.; Doughty, C.; and Bodvarsson, G.S. 1998. "An Active Fracture Model for Unsaturated Flow and Transport in Fractured Rocks." *Water Resources Research, 34*, (10), 2633-2646. Washington, D.C.: American Geophysical Union. TIC: 243012.

100161 Montazer, P. and Wilson, W.E. 1984. *Conceptual Hydrologic Model of Flow in the Unsaturated Zone, Yucca Mountain, Nevada*. Water-Resources Investigations Report 84-4345. Lakewood, Colorado: U.S. Geological Survey. ACC: NNA.19890327.0051.

105731 Neuman, S.P. 1994. "Generalized Scaling of Permeabilities: Validation and Effect of Support Scale." *Geophysical Research Letters, 21*, (5), 349-352. Washington, D.C.: American Geophysical Union. TIC: 240142.

158449 NRC (U.S. Nuclear Regulatory Commission) 2002. *Yucca Mountain Review Plan, Draft Report for Comment*. NUREG-1804, Rev. 2. Washington, D.C.: U.S. Nuclear Regulatory Commission, Office of Nuclear Material Safety and Safeguards. TIC: 252488.

100684 Pruess, K. 1987. *TOUGH User's Guide*. NUREG/CR-4645. Washington, D.C.: U.S. Nuclear Regulatory Commission. TIC: 217275.

124773 Roberson, J.A. and Crowe, C.T. 1990. *Engineering Fluid Mechanics*. 4th Edition. Boston, Massachussetts: Houghton Mifflin. TIC: 247390.

102097 Rousseau, J.P.; Kwicklis, E.M.; and Gillies, D.C., eds. 1999. *Hydrogeology of the Unsaturated Zone, North Ramp Area of the Exploratory Studies Facility, Yucca Mountain, Nevada*. Water-Resources Investigations Report 98-4050. Denver, Colorado: U.S. Geological Survey. ACC: MOL.19990419.0335.

100178 Rousseau, J.P.; Loskot, C.L.; Thamir, F.; and Lu, N. 1997. *Results of Borehole Monitoring in the Unsaturated Zone Within the Main Drift Area of the Exploratory Studies Facility, Yucca Mountain, Nevada*. Milestone SPH22M3. Denver, Colorado: U.S. Geological Survey. ACC: MOL.19970626.0351.

160355 USGS (U.S. Geological Survey) 2001. *Simulation of Net Infiltration for Modern and Potential Future Climates*. ANL-NBS-HS-000032 REV 00 ICN 02. Denver, Colorado: U.S. Geological Survey. ACC: MOL.20011119.0334.

100610 van Genuchten, M.T. 1980. "A Closed-Form Equation for Predicting the Hydraulic Conductivity of Unsaturated Soils." *Soil Science Society of America Journal, 44*, (5), 892-898. Madison, Wisconsin: Soil Science Society of America. TIC: 217327.

160401 Wang, J.S. 2002. "Scientific Notebooks Referenced in AMR U0035, Calibrated Properties Model, MDL-NBS-HS-000003 REV 01." Memorandum from J.S. Wang (BSC) to File, October 25, 2002, with attachments. ACC: MOL.20021107.0287.

106793 Wang, J.S.Y. and Narasimhan, T.N. 1993. "Unsaturated Flow in Fractured Porous Media." Chapter 7 of *Flow and Contaminant Transport in Fractured Rock*. Bear, J.; Tsang, C-F.; and de Marsily, G., eds. San Diego, California: Academic Press. TIC: 235461.

114295 Weast, R.C., ed. 1987. *CRC Handbook of Chemistry and Physics: 1987-1988*. 68th Edition. Pages A-1, F-72, F-185 only. Boca Raton, Florida: CRC Press. TIC: 245444.

154817 YMP (Yucca Mountain Site Characterization Project) 2001. *Q-List*. YMP/90-55Q, Rev. 7. Las Vegas, Nevada: Yucca Mountain Site Characterization Office. ACC: MOL.20010409.0366.

Software Cited

146536 LBNL (Lawrence Berkeley National Laboratory) 08/16/1999. *Software Routine: e9-3in V1.0*. 1.0. Sun workstation. 10126-1.0-00.

134754 LBNL (Lawrence Berkeley National Laboratory) 1999. *Software Code: infil2grid*. V1.6. PC with Windows/95 or 98. Sun or DEC Workstation with Unix OS. 10077-1.6-00.

154793 LBNL (Lawrence Berkeley National Laboratory) 2002. *Software Code: infil2grid*. V1.7. DEC-Alpha, PC. 10077-1.7-00.

160106 LBNL (Lawrence Berkeley National Laboratory) 2002. *Software Code: iTOUGH2*. V5.0. SUN UltraSparc., DEC ALPHA, LINUX. 10003-5.0-00.

160107 LBNL (Lawrence Berkeley National Laboratory) 2002. *Software Code: TBgas3D*. V2.0. SUN UltraSparc. 10882-2.0-00.

146533 LBNL (Lawrence Berkeley National Laboratory) 2002. *Software Routine: aversp_1*. V1.0. Sun workstation. 10878-1.0-00.

9.2 CODES, STANDARDS, REGULATIONS, AND PROCEDURES

10 CFR 63. Energy: Disposal of High-Level Radioactive Wastes in a Geologic Repository at Yucca Mountain, Nevada. Readily available.

AP-2.14Q, Rev. 2, ICN 2. *Review of Technical Products and Data.* Washington, D.C.: U.S. Department of Energy, Office of Civilian Radioactive Waste Management. ACC: DOC.20030206.0001.

AP-2.22Q, Rev. 0, ICN 0. *Classification Criteria and Maintenance of the Monitored Geologic Repository Q-List.* Washington, D.C.: U.S. Department of Energy, Office of Civilian Radioactive Waste Management. ACC: MOL.20020314.0046.

AP-2.27Q, Rev. 0, ICN 0. *Planning for Science Activities*. Washington, D.C.: U.S. Department of Energy, Office of Civilian Radioactive Waste Management. ACC: MOL.20020701.0184.

AP-3.15Q, Rev. 3, ICN 4. *Managing Technical Product Inputs*. Washington, D.C.: U.S. Department of Energy, Office of Civilian Radioactive Waste Management. ACC: MOL.20021105.0163.

AP-6.1Q, Rev. 7, ICN 0. *Document Control*. Washington, D.C.: U.S. Department of Energy, Office of Civilian Radioactive Waste Management. ACC: MOL.20030120.0178.

AP-17.1Q, Rev. 2, ICN 3. *Record Source Responsibilities for Inclusionary Records*. Washington, D.C.: U.S. Department of Energy, Office of Civilian Radioactive Waste Management. ACC: MOL.20020813.0054.

AP-32.4, Rev. 0, ICN 1, BSCN 1. *Records Retention and Disposition*. Washington, D.C.: U.S. Department of Energy, Office of Civilian Radioactive Waste Management. ACC: MOL.20010212.0274.

AP-SI.1Q, Rev. 3, ICN 4. *Software Management.* Washington, D.C.: U.S. Department of Energy, Office of Civilian Radioactive Waste Management. ACC: MOL.20020520.0283.

AP-SIII.3Q, Rev. 1, ICN 2. *Submittal and Incorporation of Data to the Technical Data Management System*. Washington, D.C.: U.S. Department of Energy, Office of Civilian Radioactive Waste Management. ACC: MOL.20020701.0177.

AP-SIII.10Q, Rev. 0, ICN 2. *Models.* Washington, D.C.: U.S. Department of Energy, Office of Civilian Radioactive Waste Management. ACC: MOL.20020506.0911.

AP-SV.1Q, Rev. 0, ICN 3. *Control of the Electronic Management of Information.* Washington, D.C.: U.S. Department of Energy, Office of Civilian Radioactive Waste Management. ACC: MOL.20020917.0133.

YMP-LBNL-QIP-6.1 Rev. 8, Mod. 0. *Document Review.* Berkeley, California: Lawrence Berkeley National Laboratory. ACC: MOL.20021024.0322.

YMP-LBNL-QIP-SV.0 Rev. 2, Mod. 1. *Management of YMP-LBNL Electronic Data.* Berkeley, California: Lawrence Berkeley National Laboratory. ACC: MOL.20020717.0319.

9.3 SOURCE DATA, LISTED BY DATA TRACKING NUMBER

147613 GS000308311221.005. Net Infiltration Modeling Results for 3 Climate Scenarios for FY99. Submittal date: 03/01/2000.

155891 GS000608312261.001. Shut-In Pressure Data from Boreholes UE-25 NRG#2B, UE-25 NRG#5, USW SD-9, and USW UZ-7A from 4/1/95 through 12/31/95. Submittal date: 07/05/2000.

145581 GS940208314211.008. Table of Contacts in Boreholes USW UZ-N57, UZ-N58, UZ-N59, and UZ-N61. Submittal date: 02/10/1994.

105572 GS950208312232.003. Data, Including Water Potential, Pressure and Temperature, Collected from Boreholes USW NRG-6 and USW NRG-7A from Instrumentation through March 31, 1995. Submittal date: 02/13/1995.

106756 GS951108312232.008. Data, Including Water Potential, Pressure and Temperature, Collected from Boreholes UE-25 UZ#4 & UZ#5 from Instrumentation through September 30, 1995, and from USW NRG-6 & NRG-7A from April 1 through September 30, 1995. Submittal date: 11/21/1995.

105573 GS960308312232.001. Deep Unsaturated Zone Surface-Based Borehole Instrumentation Program Data from Boreholes USW NRG-7A, USW NRG-6, UE-25 UZ#4, UE-25 UZ#5, USW UZ-7A, and USW SD-12 for the Time Period 10/01/95 through 3/31/96. Submittal date: 04/04/1996.

105974 GS960808312232.004. Deep Unsaturated Zone Surface-Based Borehole Instrumentation Program Data for Boreholes USW NRG-7A, USW NRG-6, UE-25 UZ#4, UE-25 UZ#5, USW UZ-7A and USW SD-12 for the Time Period 4/1/96 through 8/15/96. Submittal date: 08/30/1996.

106784 GS960908312261.004. Shut-in Pressure Test Data from UE-25 NRG#5 and USW SD-7 from November, 1995 to July, 1996. Submittal date: 09/24/1996.

105975 GS970108312232.002. Deep Unsaturated Zone, Surface-Based Borehole Instrumentation Program - Raw Data Submittal for Boreholes USW NRG-7A, USW NRG-6, UE-25 UZ#4, UE-25 UZ#5, USW UZ-7A, and USW SD-12, for the Period 8/16/96 through 12/31/96. Submittal date: 01/22/1997.

105978 GS970808312232.005. Deep Unsaturated Zone Surface-Based Borehole Instrumentation Program Data from Boreholes USW NRG-7A, UE-25 UZ#4, UE-25 UZ#5, USW UZ-7A and USW SD-12 for the Time Period 1/1/97 - 6/30/97. Submittal date: 08/28/1997.

105980 GS971108312232.007. Deep Unsaturated Zone Surface-Based Borehole Instrumentation Program Data from Boreholes USW NRG-7A, UE-25 UZ #4, UE-25 UZ #5, USW UZ-7A and USW SD-12 for the Time Period 7/1/97 - 9/30/97. Submittal date: 11/18/1997.

105982 GS980408312232.001. Deep Unsaturated Zone Surface-Based Borehole Instrumentation Program Data from Boreholes USW NRG-7A, UE-25 UZ #4, USW NRG-6, UE-25 UZ #5, USW UZ-7A and USW SD-12 for the Time Period 10/01/97 - 03/31/98. Submittal date: 04/16/1998.

106752 GS980708312242.010. Physical Properties of Borehole Core Samples, and Water Potential Measurements Using the Filter Paper Technique, for Borehole Samples from USW WT-24. Submittal date: 07/27/1998.

106748 GS980808312242.014. Physical Properties of Borehole Core Samples and Water Potential Measurements Using the Filter Paper Technique for Borehole Samples from USW SD-6. Submittal date: 08/11/1998.

159525 LB0205REVUZPRP.001. Fracture Properties for UZ Model Layers Developed from Field Data. Submittal date: 05/14/2002.

159526 LB0207REVUZPRP.001. Revised UZ Fault Zone Fracture Properties. Submittal date: 07/03/2002.

159672 LB0207REVUZPRP.002. Matrix Properties for UZ Model Layers Developed from Field and Laboratory Data. Submittal date: 07/15/2002.

160108 LB02081DKMGRID.001. 2002 UZ 1-D and 2-D Calibration Grids. Submittal date: 08/26/2002.

160250 LB02103DPNEUSM.001. 3-D Pneumatic Simulation (FY99). Submittal date: 10/08/2002.

125868 LB991091233129.001. One-Dimensional, Mountain-Scale Calibration for AMR U0035, "Calibrated Properties Model". Submittal date: 10/22/1999.

119902 LB991091233129.003. Two-Dimensional Fault Calibration for AMR U0035, "Calibrated Properties Model". Submittal date: 10/22/1999.

104055 LB997141233129.001. Calibrated Basecase Infiltration 1-D Parameter Set for the UZ Flow and Transport Model, FY99. Submittal date: 07/21/1999.

119933 LB997141233129.002. Calibrated Upper-Bound Infiltration 1-D Parameter Set for the UZ Flow and Transport Model, FY99. Submittal date: 07/21/1999.

119940 LB997141233129.003. Calibrated Lower-Bound Infiltration 1-D Parameter Set for the UZ Flow and Transport Model, FY99. Submittal date: 07/21/1999.

153777 MO0012MWDGFM02.002. Geologic Framework Model (GFM2000). Submittal date: 12/18/2000.

155989 MO0109HYMXPROP.001. Matrix Hydrologic Properties Data. Submittal date: 09/17/2001.

9.4 OUTPUT DATA, LISTED BY DATA TRACKING NUMBER

LB0208UZDSCPLI.001. Drift-Scale Calibrated Property Sets: Lower Infiltration Supporting Files. Submittal date: 08/27/2002.

LB0208UZDSCPLI.002. Drift-Scale Calibrated Property Sets: Lower Infiltration Data Summary. Submittal date: 08/26/2002.

LB0208UZDSCPMI.001. Drift-Scale Calibrated Property Sets: Mean Infiltration Supporting Files. Submittal date: 08/27/2002.

LB0208UZDSCPMI.002. Drift-Scale Calibrated Property Sets: Mean Infiltration Data Summary. Submittal date: 08/26/2002.

LB0208UZDSCPUI.001. Drift-Scale Calibrated Property Sets: Upper Infiltration Supporting Files. Submittal date: 08/27/2002.

LB02091DSSCP3I.001. 1-D Site Scale Calibrated Properties: Supporting Files. Submittal date: 09/18/2002.

LB02091DSSCP3I.002. 1 -D Site Scale Calibrated Properties: Data Summary. Submittal date: 09/18/2002.

LB02092DSSCFPR.001. 2-D Site Scale Calibrated Fault Properties: Supporting Files. Submittal date: 09/18/2002.

LB02092DSSCFPR.002. 2-D Site Scale Calibrated Fault Properties: Data Summary. Submittal date: 09/18/2002.

LB0210AMRU0035.002. Model Validation and Parameter Uncertainty: Data Summary. Submittal date: 10/10/2002.

LB0302AMRU0035.001. Model Validation and Parameter Uncertainty: Supporting Files. Submittal date: 02/07/2003.

LB0302UZDSCPUI.002. Drift-Scale Calibrated Property Sets: Upper Infiltration Data Summary. Submittal date: 02/05/2003.

INTENTIONALLY LEFT BLANK

10. ATTACHMENTS

Attachment I – Description of Excel Files

INTENTIONALLY LEFT BLANK

ATTACHMENT I — DESCRIPTION OF EXCEL FILES

layavsat.xls (Output-DTN: LB0208UZDSCPMI.001**)**

This Excel file was used to calculate and format saturation data for iTOUGH2 V.5.0 (LBNL 2002 [160106]). All the relevant input and output files (including the Excel file itself) were submitted to TDMS under DTN: LB0208UZDSCPMI.001).

In worksheets "***sat", *** corresponds to the borehole name. Columns C-G were imported from files "***.out". These files with the extension "out" are output files from runs of aversp_1 V 1.0 (LBNL 2002 [146533])and listed in Output-DTN: LB0208UZDSCPMI.001. Columns H, I, and J contain the standard error, handling error, and the total error. The formulations used for calculating these errors are Equations (1), (2) and (6) (Section 6.2.2). Columns A and B contain the corresponding element names and material types that were imported from file m1di8m.dkm (Output-DTN: LB0208UZDSCPMI.001). Columns A, B, F, and J were copied from worksheets "***sat" to columns B, D, E and F, respectively, in worksheet "iTOUGH2 pre-input" below Row 7. Rows 1 to 7 are iTOUGH2 input format. Worksheet "iTOUGH2 input" was determined from "iTOUGH2 pre-input". Information in Column B in "iTOUGH2 input" was copied from Columns B, C, E, and F in "iTOUGH2 pre-input". The worksheet "iTOUGH2 input" is the final output of this Excel file.

in_situ_pcap.xls (Output-DTN: LB0208UZDSCPMI.001**)**

This excel file was used for data reduction for water potential data and formatting for iTOUGH2 V 5.0 (LBNL 2002 [160106]) input. It was modified from file in_situ_pcap2.xls from DTN: LB991091233129.001 [125868], and submitted to TDMS under DTN: LB0208UZDSCPMI.001.

In worksheet "iTOUGH2 trans," columns A to G are from in_situ_pcap2.xls, and Columns I to O were copied from numerical grid file "m1di5m.dkm.nvf.SP.nt" (Output-DTN: LB0208UZDSCPMI.001). The appropriate element names and the corresponding information (Columns I to O) were determined by comparing borehole information given in "Boreholes.mck" (DTN: LB02081DKMGRID.001 [160108]), numerical grids "m1di5m.dkm.nvf.SP.nt" and elevations given in Column C.

In worksheet "iTOUGH2 pre-input", Columns B, D, and F (below row 9) were copied from Columns I, E and J in "iTOUGH2 trans," respectively. Column E is the data in Column D times 10E5 (i.e., converting from bars to Pa). The uncertainty of the data is calculated in Column G as the logarithmic equivalent of ± 1.0 bars:

$$SE_{\log(\psi)} = \frac{\log(|\psi| + 1bar) - \log(|\psi| - 1bar)}{2} \qquad \psi > 1 \text{ bar}$$

$$SE_{\log(\psi)} = \log(|\psi| + 1bar) - \log(|\psi|) \qquad \psi \leq 1 \text{ bar}$$

Worksheet "iTOUGH2 input" was determined from "iTOUGH2 pre-input". Information in Column B in "iTOUGH2 input" was copied from Columns B, C, E, and G in "iTOUGH2 pre-input". The worksheet "iTOUGH2 input" is the final output of this Excel file.

UZ-7asat1_02.xls (Output-DTN: LB02092DSSCFPR.001)

Gridblock-averaged saturation data for UZ-7a are determined using Excel file: UZ-7asat1_02.xls that is modified from UZ-7asat.xls in DTN: LB991091233129.003 [125868]. The averaged saturation data were used for calibrating fault properties. The Excel file was submitted to TDMS under DTN: LB02092DSSCFPR.001.

Worksheet "data" contains saturation measurements contained in UZ-7asat.xls in DTN: LB991091233129.003 [119902]. Because grid mesh is only approximately consistent with the geology of the UZ-7a borehole, some correction is needed for calculating gridblock-averaged saturations:

The top elevation for UZ-7a is 4230 ft=4230 *0.3048 (m)=1289.3 m (from contacts00md.dat of DTN: MO0012MWDGFM02.002 [153777]). The top elevation from the grid is 1291.8 m (from EWUZ7a.mck of DTN: LB02081DKMGRID.001 [160108]). Note that in worksheet "fault_grid" of UZ-7asat1_02.xls, elevation information comes from EWUZ7a.mck. The small elevation difference is ignored. In other words, the top of grid is considered to correspond to depth =0 in worksheet "data".

The thickness of a geological layer in "data" may be not exactly the same as that in the grid. To map the data to grid elevations, some corrections are needed. In one of the worksheets "ftcw", "fptn", "ftsw", "nftptpul", "nftptpmn" and "nftptpll", Column A contains three numbers. From top to bottom, they are top and bottom depths of the corresponding geologic unit and the difference between them (the thickness of the unit), respectively. They are determined from worksheet "data". Note that the depth of contacts between subgeological layers in worksheet "data" is calculated as average depth of two closest sample locations within the corresponding sublayers. Columns B and C were copied from "fault grid". Column D contains depth values that were calculated as depths minus the top depth of the unit. The bottom number in this column is the thickness of the unit in the grid. Columns K, L, and N were copied from worksheet "data". Column M contains corrected depths that were calculated by

[(depth in Column L – depth at Cell A2) x thickness in grid]/ (thickness calculated from "data")

Column E contains numbers of samples within the gridblock (determined by the top and bottom depth values of the element (Column D) and the sample depth values in Column M). Columns F to G are mean saturation, standard deviation, standard error, measurement error, and total error, respectively. The formulations used for calculating these errors are Equations (1), (2) and (6) (Section 6.2.2). The mean saturation and total error were used in iTOUGH2 V5.0 (LBNL 2002 [160106]) input for the corresponding element (Column B).

QAd.xls (Output-DTN: LB02091DSSCP3I.001)

This excel file was used to determine F values (Equation (8)). It was submitted to TDMS under DTN: LB02091DSSCP3I.001).

Input files for Qad.xls are one of the files MGasi.tec, LGasi.tec and UGasi.tec (output DTN: LB02091DSSCP3I.001). Delete lines 1-3041 and then delete lines 122-244 from one of these files with the extension tec. (To calculate F value for the observed data, delete lines 1-1919 and then 122-244 from one of these files.) Then, copy the file to Columns A and B in QAd.xls. Copy B1 to C1-121, and Copy B122 to C122 – 242. In Column D, D1-121 correspond to (Bi-Ci) (i=1,121). In Column E, E1-121 correspond to (Bj-Cj) (j=122-242). In Column F, F1-121 correspond to $(Di-Ei)^2$ for i=1 to 121. Cell G1 contains summation of Fi for i =1 to 121. Cell H1 contains $(G1)^{0.5}/121$, or the F value in Equation (8).

Verification.xls (Output-DTN: LB0302AMRU0035.001)

This file was used for processing data for model validation in terms of matrix saturation and water potential data (Section 7). All data files mentioned below were submitted to TDMS under DTN: LB0210AMRU0035.001.

Copy "Residual Analysis" sections from: LVerify_Ci.out, MVerify_Ci.out, and UVerify_Ci.out into Verification.xls as Worksheets "LVerify_Ci", "MVerify_Ci", and "UVerify_Ci", respectively. In the worksheet known as "Overall", list the boreholes that were used in calibration and the boreholes that were saved for verification purpose separately. In each individual worksheet (LVerify_Ci, MVerify_Ci, and UVerify_Ci), calculate the square of the residual (Measured-computed, column I) for each data point in column P (e.g., enter (I14)^2 in P14). Then calculate the root-mean-square error for each group, saturation in the boreholes used in calibration (P1), Saturation in the boreholes not used in calibration (P2), Capillary pressure in the boreholes used in calibration (Q1), and capillary pressure in the boreholes not used in calibration (Q2), using standard functions SQRT and AVERAGE. In Cell P1, enter "= SQRT(AVERAGE(P14:P142, P191:P288, P302:P327, P330:P339, P364:P366, P373:P375))". In Cell P2, enter "= SQRT(AVERAGE(P143:P190, P289:P301, P328:P329, P340:P363, P367:P372))" In Cell Q1, enter "= SQRT(AVERAGE(P381:P411))" In Cell Q2, enter "=SQRT(AVERAGE(P376:P380))" Summarize the above results into two tables, saturation (D1-G5) and capillary pressure (D17-G21) on worksheet 'Overall', respectively. In particular,

Cell E2, enter "=+LVerify_Ci!P2"	--Calibration
Cell E3, enter "=+LVerify_Ci!P3"	--Prediction
Cell E4, enter "=3*E2"	--Criteria
Cell F2, enter "=+MVerify_Ci!P2"	--Calibration
Cell F3, enter "=+MVerify_Ci!P3"	--Prediction
Cell F4, enter "=3*F2"	--Criteria
Cell G2, enter "=+UVerify_Ci!P2"	--Calibration
Cell G3, enter "=+UVerify_Ci!P3"	--Prediction
Cell G4, enter "=3*G2"	--Criteria
Cell E18, enter "=+LVerify_Ci!Q2"	--Calibration
Cell E19, enter "=+LVerify_Ci!Q3"	--Prediction
Cell E20, enter "=3*E18"	--Criteria
Cell F18, enter "=+MVerify_Ci!Q2"	--Calibration
Cell F19, enter "=+MVerify_Ci!Q3"	--Prediction
Cell F20, enter "=3*F18"	--Criteria
Cell G18, enter "=+UVerify_Ci!Q2"	--Calibration

Cell G19, enter "=+UVerify_Ci!Q3" --Prediction
Cell G20, enter "=3*G18" --Criteria

VGas.xls (Output-DTN: LB0302AMRU0035.001)

This file was used for processing data for model validation in terms of gas pressure data (Section 7). All data files mentioned below were submitted to TDMS under DTN: LB0210AMRU0035.001.

Copy vLGasi.tec, vMGasi.tec, vUGasi.tec, Nli.tec, Nmi.tec, and Nui.tec into vGas.xls as worksheets "vLGasi", "vMGasi", "vUGasi", "Nli", "Nmi", and "Nui", respectively. Calculate the square errors (e.g., =+(C4-C165)^2 in I4) on the column I on worksheets "vLGasi", "vMGasi", and "vUGasi". The related cells are:

Borehole	Cells
USW NRG-7a	I4-I163; I326-I485; I648-I807; I970-I1129
USW SD-12	I3056-I3215; I3378-I3537; I3700-I3859; I4022-I4181
USW SD-7	I4344-I4503; I4666-I4825; I4988-I5147; I5310-I5469

For each section above, the first half contains the data used in calibration and the second half contains the data not used in calibration. Therefore, calculate the average values for each part of each section separately and put them in the following cells (in the order of the above sections):

Calibration	Prediction
K4	L4
K326	L326
K648	L648
K970	L970
K3056	L3056
K3378	L3378
K3700	L3700
K4022	L4022
K4344	L4344
K4666	L4666
K4998	L4998
K5310	L5310

The calculation uses standard function AVERAGE, e.g., in Cell K4, enter "=AVERAGE(I4:I83)" and in Cell L4, enter "=AVERAGE(I84:I163)".

Calculate the overall root mean square errors in Cells K2 and L2 using standard functions SQRT and AVERAGE for calibration and prediction, respectively. In Cell K2, enter "=SQRT(AVERAGE(K4:K65536))". In Cell L2, enter "=SQRT(AVERAGE(L4:L65536))". In Cell M2, calculate the number of data points by using standard function COUNT (i.e., enter "=COUNT(I4:I5469)/2"). Note that, in MS Excel, only those cells having data participate in the calculation using either AVERAGE or COUNT. Dividing by 2 in Cell M2 is required because half data are used for either calibration or prediction.

For worksheets NLi, NMi, and NUi (NRG6), all data were not used in calibration and the second set of calculated data (SIM1) is the final result. Therefore, the square errors of prediction are calculated in cells:
I4-I105, I210-I130, I454-I574, and I698-I818 (e.g., enter "=+(C4-C942)^2" in Cell I4).

Calculate the root mean square error in Cell J2 (i.e., enter "=SQRT(AVERAGE(I4:I818)")) and the number of data points in Cell K2 (i.e., enter "=COUNT(I4:I818)"), respectively.

Summarize the calibration and prediction errors on Cells A6-E9 of the worksheet 'Summary' in vGas.xls. The calibration errors are from cell K2 in worksheets "vLGasi", "vMGasi", and "vUGasi". The prediction errors are calculated as the averages of the prediction errors of the 30 days after calibration in the same boreholes and the USW NRG-6 (no data used in calibration). Because the numbers of data points are different in the two data sets, the average values are calculated using the numbers of data points in each data set as weighting factors. The detailed calculations are as follows:

Cells	Formula
B7	=+vLGasi!K$2
B8	=+vMGasi!K$2
B9	=+vMGasi!K$2
C7	=+(vLGasi!L2*vLGasi!M2+NLi!J2*NLi!K2)/(vLGasi!M2+NLi!K2)
C8	=+(vMGasi!L2*vMGasi!M2+NMi!J2*NMi!K2)/(NMi!K2+vMGasi!M2)
C9	=+(vUGasi!L2*vUGasi!M2+NUi!J2*NUi!K2)/(NUi!K2+vUGasi!M2)
D7	=+B7*3
D8	=+B8*3
D9	=+B9*3

Record time period is relevant to the calibration and prediction (validation) on worksheet "Summary" (H3-K6) based on the input files: vLGasi, vMGasi, vUGasi, NLi, NMi, and NUi. Note that borehole USW NRG-5 has been excluded in the validation because no measured data were available beyond the calibration period. For borehole USW NRG-6, only 25 days of measured data were available for the sensor located at layer Tpcpln, starting from 04/01/1995.